Physics Characterization of TLD-600 and TLD-700 and Acceptance Testing of New X-RAD 160 Biological X-Ray Irradiator

by

Yanan Cao

Graduate Program in Medical Physics
Duke University

Date:_____

Approved:

_____
Terry Yoshizumi, Supervisor

_____
Rathnayaka Gunasingha

_____
James Colsher

Thesis submitted in partial fulfillment of
the requirements for the degree of Master of Science in the
Graduate Program in Medical Physics
in the Graduate School
of Duke University

2013

ABSTRACT

Physics Characterization of TLD-600 and TLD-700 and Acceptance Testing of New X-RAD 160 Biological X-Ray Irradiator

by

Yanan Cao

Graduate Program in Medical Physics
Duke University

Date:_____

Approved:

_____
Terry Yoshizumi, Supervisor

_____
Rathnayaka Gunasingha

_____
James Colsher

An abstract of a thesis submitted in partial
fulfillment of the requirements for the degree
of Master of Science in the Graduate Program in Medical Physics
in the Graduate School of
Duke University

2013

Abstract

Project 1: Physics characterization of TLD-600 and TLD-700

Purpose:

It is suggested that a pair of TLD-600 and TLD-700 can measure the exposure in neutron-photon mix fields. However the basic information of physics characterization of TLD-600 and 700 is not available. The purpose of this work was to study the individual TLD variation and the energy dependence of TLD-600 and TLD-700.

Methods:

The individual calibration factors for 52 TLD-600 chips and 51 TLD-700 chips were determined under x-ray beams of 60 kVp, 80 kVp, 120 kVp, a mono-energetic 662 keV gamma beam of a Cs-137 source, and an Am-Be neutron beam (4.4 MeV). The individual calibration factor was calculated as the ratio of the group average response in μC/mR and the individual response inμC/mR. In addition, energy corrections factors for the individual calibration factors were determined, from each of the x-ray beams (60 kVp, 80 kVp and 120 kVp) to the 662 keV Cs-137 gamma beams.

Results:

For TLD-600, the range and relative standard deviation of the individual calibration factors are: 60 kVp (0.94003-1.0927, 3.5369%), 80 kVp (0.9395-1.0867, 3.0952%), 120 kVp (0.83403-1.0796, 4.5732%), 662 keV (0.80465-1.1926, 9.2515%), AmBe (0.91740-

0.94905, 3.0882%); and the energy corrections factors relative to the 662 keV Cs-137 beams are: 1.2223 (60kVp), 1.1013 (80kVp), 1.0299 (120kVp).

For TLD-700 the range and relative standard deviation of the individual calibration factors are: 60 kVp (0.94351-1.0630, 2.6044%), 80 kVp (0.91690-1.0614, 2.6996%), 120 kVp (0.95697-1.0474, 2.3606%), 662 keV (0.91348-1.2270 , 4.2243%), AmBe (0.79330-1.2268 , 9.1577%); and the energy corrections factors relative to the 662 keV Cs-137 beams are: 1.0373 (60kVp), 0.97661 (60kVp), 0.88532 (60kVp).

Conclusion:

We have measured individual calibration factors and the average energy correction factors for photon beams and Am-Be neutron beams. Our results will be used in the future experiments and measurements with TLD-600 and TLD-700.

Project 2: Acceptance testing of new X-RAD 160 Biological X-Ray Irradiator

Purpose:

An X-RAD 160 Biological X-Ray Irradiator was recently installed at Duke University to serve as a key device for cellular radiobiology research. The purpose of this study is to perform acceptance testing on the new irradiator for operator radiation safety and irradiation specifications.

Methods:

The acceptance testing included the following tests: (1) Leakage radiation survey, (2) Half-value layer (beam quality), (3) Uniformity, (4) KVp accuracy, (5) Exposure at

varying mA (linearity of mA), (6) Exposure at varying kVp, (7) Inverse square measurements, (8) Field size measurement, and (9) Exposure constancy.

The irradiation parameters for the first round of acceptance testing performed on September 21, 2012 were: Leakage radiation survey (none, 160 kVp, 18 mA, 200s), Beam quality (40cm, 50-140 kVp in 10 kVp incensement, 1 mA, 10s, none), Uniformity (40cm, 160 kVp, 18 mA, 15s, F1), KVp accuracy (40cm, 50-150 kVp in 10 kVp incensement, 10 mA, 15s, none), Linearity of mA (40cm, 160 kVp, 2-18 mA, 15s, none), Inverse square measurements (20-63cm, 160 kVp, 1mA, 30s, none), Field size measurement (40cm, 160 kVp, 10 mA, 15s, none), and Exposure constancy (40cm, 160 kVp, 18 mA, 20s, none).

The irradiation parameters for the second round of acceptance testing performed on November 18, 2012 were: Beam quality (40cm, 35-150 kVp, 1 mA, 10s, F1) , KVp accuracy (40cm, 35-150 kVp, 1 mA, 10s, F1), Variation of kVp (40cm, 160 kVp, 18 mA, 30s, F1), Linearity of mA (40cm, 160 kVp, 1-18 mA, 30s, F1), Uniformity (40cm, 160 kVp, 18 mA, 30s, F1), and Inverse square measurements (20-63cm, 160 kVp, 18 mA, 30s, F1).

Results:

The first round of acceptance testing performed on September 21, 2012 failed due to the fact that the measured exposure along the X-axis was significantly non-uniform; the exposure greatly decreases going in the left direction, which is a clear indication of un-corrected anode heel effect. After the X-ray tube was returned to the manufacturer, the beam was reconfigured by tilting the X-ray tube. Another round of acceptance

testing was performed on December 18, 2012. The results of second round of acceptance testing showed there was no radiation hazard for the researcher surrounding the new X-RAD 160 Biological X-Ray Irradiator and the machine had a uniform and consistent beam.

Conclusion:

The acceptance testing fulfilled the initial purpose. A major problem was found and corrected. The machine is currently used normally in the following experiments; routine maintenance and quality assurance (QA) are required.

Contents

List of Tables

List of Figures

Acknowledgements

I would like to acknowledge the following Duke faculties and students, for their contributions and help. Without their kind support and advice, I would not have been able to complete this thesis. I would also like to express my thanks for stipend support from Duke Radiation Dosimetry Laboratory.

- Terry Yoshizumi Ph.D. Professor
- Rathnayaka Gunasingha Ph.D. Faculty in Medical Physics
- James Colsher Ph.D. Adjunct Assistant Professor
- Giao Nguyen M.S.
- Chu Wang Ph.D. student
- Natalie Ann Januzis Ph.D. student
- Anna Rodrigues Ph.D. student

Finally, I would like to express my deepest thanks to my parents for their infinite love and support they have provided.

1. Introduction

1.1 Overview

There are two research projects related to radiation dosimetry discussed respectively in this thesis: 1) Physics characterization of TLD-600 and TLD-700 and 2) Physics characterization of a new orthovoltage X-ray irradiator.

Radiation dosimetry is the process of measuring and analyzing the radiation dose to the medium [1].

In this section, basic quantities and units in radiation dosimetry; the basic principles of radiation detectors used in the studies in this thesis will be discussed.

1.2 Basic Quantities and Units in radiation Dosimetry

Several basic quantities and units of radiation dosimetry are introduced in this section. These Quantities include exposure, absorbed dose, and the f-factor.

Exposure, X is defined as the total charge liberated per unit mass in a small volume of air of mass by photon beams less than about 3MeV. The unit is coulomb per kilogram (C/kg) or roentgen [1].

$$X = \frac{Q}{m} \tag{1-1}$$

Absorbed Dose, D is defined as the energy deposited per unit mass from any kind of ionizing radiation in absorber medium [1].

$$X = \frac{\mathrm{d}\varepsilon}{\mathrm{dm}} \tag{1-2}$$

where dε is energy absorbed by ionizing radiation to material, m is a finite mass. The unit of absorbed dose is Gray (Gy) (SI) or rad (old).

The f-factor is a unit used to convert exposure in air to absorbed dose in a material.

$$f = 0.87 \frac{\left(\frac{\mu_{en}}{\rho}\right)_{material}}{\left(\frac{\mu_{en}}{\rho}\right)_{air}} \; rad \qquad 1\text{-}3$$

where quantity$\left(\frac{\mu_{en}}{\rho}\right)_{material}$ is called the mass absorption attenuation coefficient of the material of choice, $\left(\frac{\mu_{en}}{\rho}\right)_{air}$ is the mass absorption attenuation coefficient of air, and f is the f-fator[1].

1.3 Ionization Chamber

Due to the low cost, relative energy independence and simplicity in usage, the ionization chamber is the most widely used radiation detectors in performing measurement of the ionizing radiation.

A schematic diagram of ionization chamber is shown in Figure 1.1. When radiation passes through the medium (gaseous, solid, or liquid, most often gaseous), it produces ion pairs in the medium. The positive ions and negative electrons then move to the cathode and anode, respectively. An electrometer can detect the ionization current created by this process. The accumulated charge is proportional to the total number of ion pairs generated by the radiation, and hence proportional to the radiation dose.

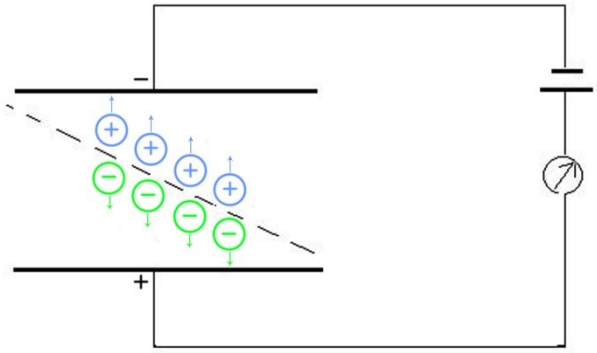

Figure 1.1: Schematic diagram of ionization chamber

In the two studies in this thesis, a 6cc ionization chamber (10x5-6, Radcal, Monrovia, CA) and a 0.18 cc ionization chamber (10x5-0.18, Radcal, Monrovia, CA) were used. They were calibrated with a NIST traceable source and standard calibrated photon beams at the University of Wisconsin on August 4st, 2011 and August 11st, 2012, respectively.

1.4 Thermoluminescent Dosimeter (TLD)

The TLD is another type of radiation dosimeter used for measuring the ionizing radiation in monitoring and research field. Lithium fluoride with impurities is the most common crystal lattice of TLD used for recording the gamma and neutron exposure. TLDs are tissue equivalent and reusable [1].

As shown in Figure 1.2, when ionizing radiation interacts with the TLD, it deposits all or part of the energy in the material. Some of the atoms in the TLD can

produce free electrons from the valence band and holes which are areas that lack electrons after absorbing enough energy. The impurities in the crystal lattice can trap the free electrons and lock them in the crystal. The crystal structure release the trapped the electrons after being heated to a certain temperature. The released electrons return to the valance band, releasing the energy receiving from the ionization as photons. Holes can also produce photons in an analogous process. The photons can be counted by using a photomultiplier tube. The total number of the photons detected is proportional to the number of trapped electrons and holes, and hence is proportional to ionizing radiation as well [2].

In this work, TLD-600 and TLD-700 were used. Both TLD-600 and TLD-700 are made of lithium fluoride (LiF) which represents a tissue equivalent material [3]. The effective Z is 8.2 for both TLD-600 and TLD-700 [3]. Both types of TLDs can measure from 10 μGy to 100Gy [3]. The difference between TLD-600 and TLD-700 is the proportion of Li-6 and Li-7 in the LiF material. While TLD-600 is made up of 95.62% of ^{6}LiF which has a large cross section for neutron and 4.38% of ^{7}LiF, TLD-700 is made up of 0.007% of ^{6}LiF and 99.993% of ^{7}LiF [3].TLD-600 can measure the photon beams and thermal neutron beams due to the 942 barn (or 9.42×10^{-26} m^2) cross section of the ^{6}Li(n,α)^{3}H reaction which means the probability of interaction between the neutron and the absorber is very high. However TLD-700 can only detect the photon beam in the low and intermediate energy range [3].

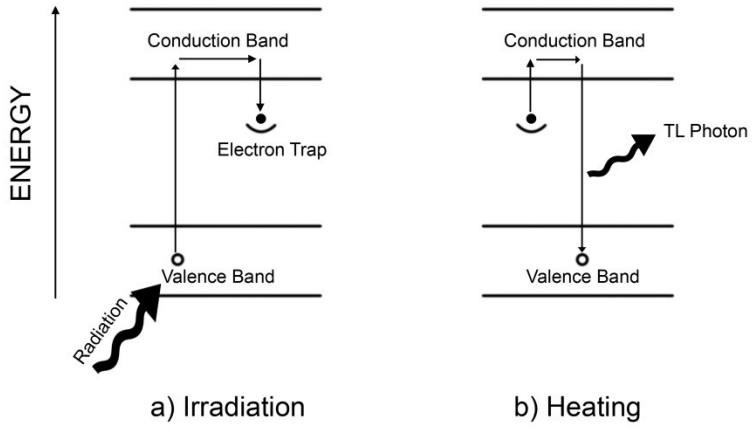

Figure 1.2: An energy level diagram illustrating the principle of TLD

1.5 Piranha Detector

The Piranha detector (RTI Electronics, Fairfield, NJ) used for X-ray QA, can measure the X-ray beam quality for various energies in air. It has a sensitive detector equipped with Bluetooth, and a range of approximately 100 meters free in air [4]. It can be used for the measurement of the half value layer (HVL), time, total filtration, and kVp [4]. In addition, it can measure at low signal levels which are an advantage for this project due to the shielding of the cabinet. The result can instantly be shown in either a PC or specific browser software after each exposure [4].

A Piranha detector placed on the shelf is shown in Figure 1.3.

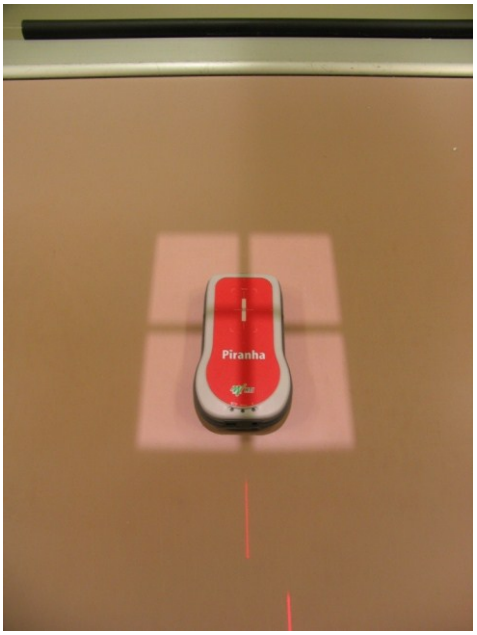

Figure 1.3: Piranha detector in X-ray beam

1.6 Geiger Muller Counter

The Geiger Muller Counter is a gas-filled radiation counter that can indicate the presence of ionizing particles. The principle of Geiger Muller Counter is similarly to the ion chamber except the voltage carried on the detectors [1]. Geiger Muller Counter cannot identify the type or energy of ionizing radiation and is usually used as a means of determining the presence of radioactivity due to the high sensitivity to ionizing radiation [1].

1.7 Radiochromic films

The radiochromic films (Gafchromic® EBT 2, International Specialty Products, Wayne, New Jersey) are used as one type of radiation dosimeter for industrial and

medical applications. Radiochromic film consists of a single or double layer of radiation-sensitive organic microcrystal monomers [5]. When radiation interacts with the film, the color of the radiochromic films turns to a shade of blue [5]. The darkness of the film increases with increasing absorbed dose. The major advantages of radiochromic films are no processing is required to develop or fix the image and high resolution [5].

2. Physics characterization of TLD-600 and TLD-700 with photon and neutron beams

2.1 Introduction

The purpose of this work was to study the individual TLD variation and the energy dependence of TLD-600 and TLD-700. The ultimate goal was to test the feasibility of quantifying gamma and neutron radiations using TLD-600 and TLD-700 at Triangle Universities Nuclear Laboratory (TUNL), Duke University.

It is suggested that a pair of TLD-600 and TLD-700 can measure the exposure in neutron-photon mix fields [6]. Once the basic information of physics characterization of TLD-600 and TLD-700 is determined.

Three accelerator facilities are operated in TUNL for nuclear physics research: the High Intensity Gamma-Ray Source (HIGS), the Tandem Accelerator Laboratory and the Laboratory for Experimental Nuclear Astrophysics. Two primary photon beams are available in HIGS: a photon beam with energies from 2 to 60 MeV and an optical beam of wavelength from infrared (IR) to Vacuum Ultraviolet (VUV) [7]. A neutron time-of-flight target room is located in the Tandem Accelerator Laboratory. The energies of neutron beam produced in neutron time-of-flight target room are 8-14 MeV [8]. Currently, neutron radiation is monitored by white Polyethylene "Rem Balls" which simulate a human body's response to neutrons with BF3 tubes inside and gamma radiation is monitored by small Tan Metal Boxes Mounted on the walls which contain a

Geiger Muller Tube [5]. It will be beneficial to have additional detectors to monitor the radiation dose at these facilities

TLDs in general have individual various responses. For example, the responses of 52 chips of TLD-700 might be not same to 60 kVp photon beams. In addition, the energy responses of TLDs to various photon energies for same amount of radiation might be different. Both characteristics are important to obtain a consistent and accurate measurement.

This study would provide the physics characterization of TLD-600 and TLD-700 for the future experiments and measurements in TUNL.

2.2 Materials and Methods

2.2.1 TLD-600 and TLD-700 and Calibration with Ionization Chamber

2.2.1.1 TLD-600 and TLD-700

In this study, 52 chips of TLD-600 and 51 chips of TLD-700 from Thermo Scientific Corporation (Hampton, New Hampshire) were used. Each TLD was assigned a unique number that was used in all the studies. Both TLD-600 and TLD-700 chips numbered 1-50 were kept in two holders. TLD-600 chips numbered 51 and 52 and TLD-700 chip number 51 were held in three separated containers which were marked with the corresponding number and type. The dimension of TLD chips was 0.3175 cm x 0.3175 cm x 0.0889 cm [3]. Some TLD chips in a holder and separated containers are displayed in Figure 2.1 and Figure 2.2.

Figure 2.1: Containers for keeping TLDs.

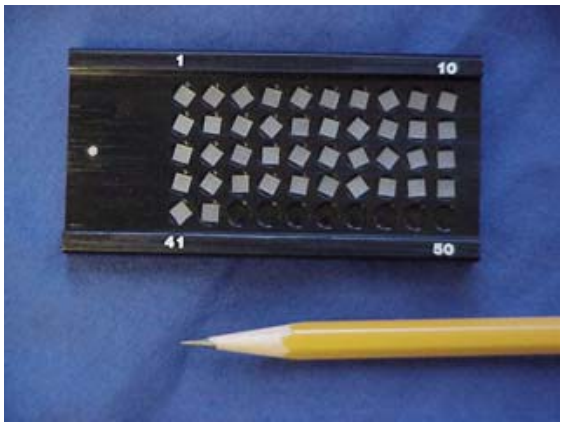

Figure 2.2: TLDs in a holder

2.2.1.2 Calibration of TLD-600 and TLD-700

A 6cc ionization chamber (10x5-6, Radcal, Monrovia, CA) calibrated by University of Wisconsin on August 4st, 2011 was used to calibrate the 52 chips of TLD-600 and 51 chips of TLD-700. A Plexiglas frame was fabricated for placement of ionization chamber and TLDs. The dimension of the frame was 20cm long, 20 cm wide and 2cm high. There is a 3.2 cm diameter semicircular hole in the middle of one side of the frame which is for the placement of ionization chamber. The chamber then was

surrounded by 50 0.5cm diameter holes for TLDs placement (Figure 2.3). Because the number of holes is less than the total number of TLDs for TLD-600 and TLD-700, TLD-600 and TLD-700 were irradiated three times. The placement of irradiation for extra TLDs was shown in Figure 2.4. The reason that these locations were chosen was that they were closer to the ionization chamber than other locations. Each TLD was placed in the hole in order corresponding to the number assigned.

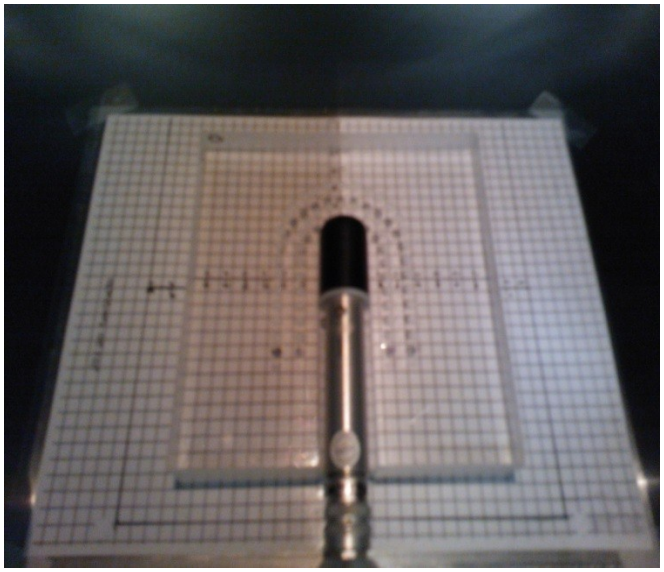

Figure 2.3: TLDs and ionization chamber in Plexiglas frame

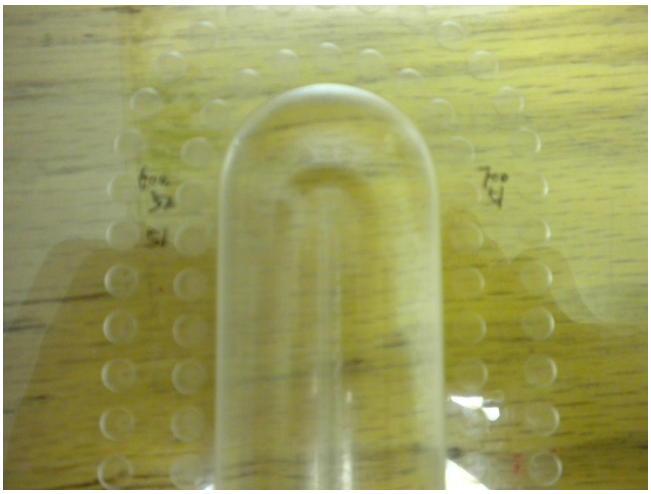

Figure 2.4: The placement of irradiation of extra TLDs.

2.2.1.3 Annealing and reading process for TLD-600 and TLD-700

Before the first and after each use, TLDs must be annealed to release electrons that may still be trapped in electron traps. The TLDs were placed in an aluminum tray used for annealing and the number of each chips was recorded, see Figure 2.5. Figure 2.6 shows one Radiation Products Design TLD Annealing Furnace (Model No. 168-001). This is done to erase TLD dose memory and prepare them for subsequent irradiation. Per manufacturer recommendation, the standard annealing procedure of LiF:Mg,Ti material (TLD-100, TLD-600, TLD-700) is a two temperature process. It is performed using two separate ovens with each oven set to one of the two temperatures. The first step is 400°C for one hour; after cooling down, the second step is 100°C for two hours [3].

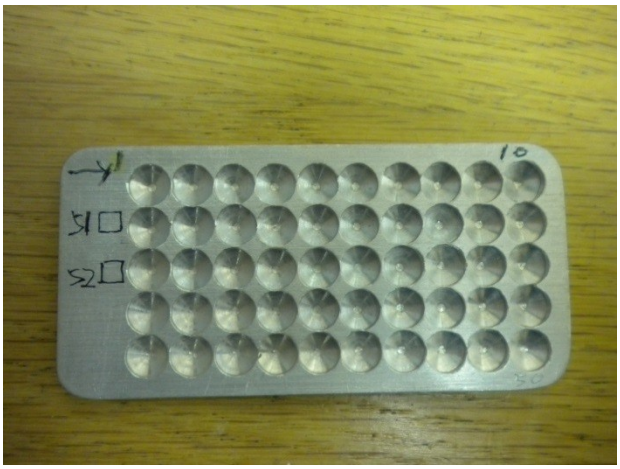

Figure 2.5: Aluminum tray used for annealing TLDs

Figure 2.6: A picture of TLD Annealing Furnace

After exposing the TLDs to radiation, a resting period of 24 hours is be required to stabilize prior to reading [9]. Harshaw Model 5500 Automatic TLD Reader (Figure 2.7) from Thermo Scientific Corporation with WinREMS™ (Figure 2.8) software was used to read the TLDs. For different types of TLDs, there are different variations required when reading the TLDs. The key difference is the Time-Temperature Profile (TTP) in this

software. According to the manufacturer, the TTPs vary different types of TLDs. The TTP settings for TLD-600 and TLD-700 are listed in Appendix A provided by Thermo Scientific Inc [10]. The procedure of reading TLDs is shown in Appendix B.

Figure 2.7: Harshaw Model 5500 Automatic TLD Reader

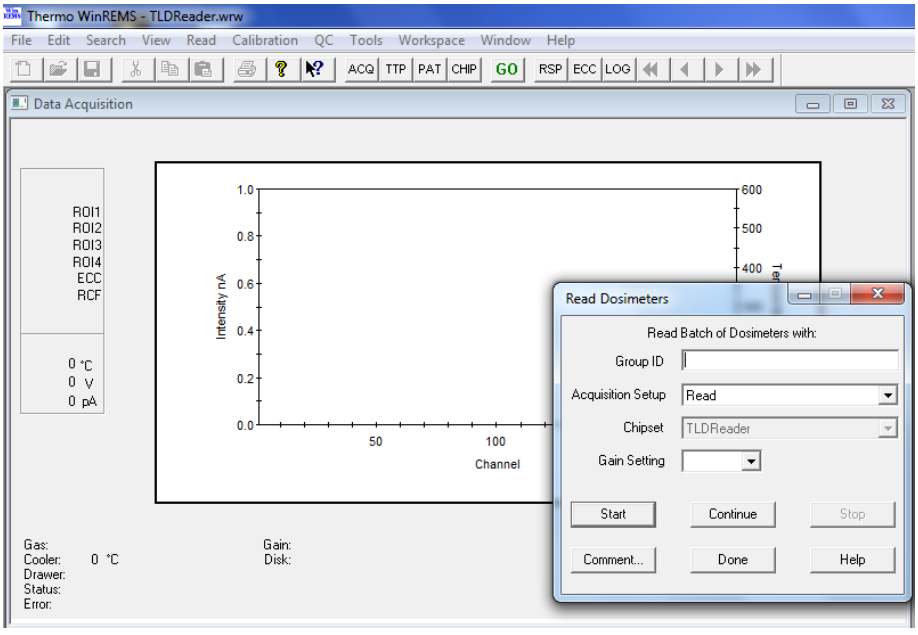

Figure 2.8: The interface of WinREMS

2.2.2 X-RAD 320 Biological X-Ray Irradiator and Radiation Parameters

The X-RAD 320 Biological X-Ray Irradiator (Precision X-RAY) in Genome Science Research Building II (GSRB II), Duke University was studied. The x-ray tube of this irradiator is displayed in Figure 2.9. The X-ray tube has a single source and it can produce a rectangular beam. The beam energies are from 5 to 320 kVp and the field sizes from 0 x 0 to 20 x 20 cm^2. Two types of removable filter: F1 (2 mm Aluminum) and F4 (0.1mm Cu + 2.5 mm Al) can be used in this machine [11]. The result of added filtration is to increase effective energy and reduce the intensity of x-ray. In this study F4 filter was used, because of its lower exposure rate than that of the F1 filter, and hence a longer radiation time leading to a more precise dose measurement.

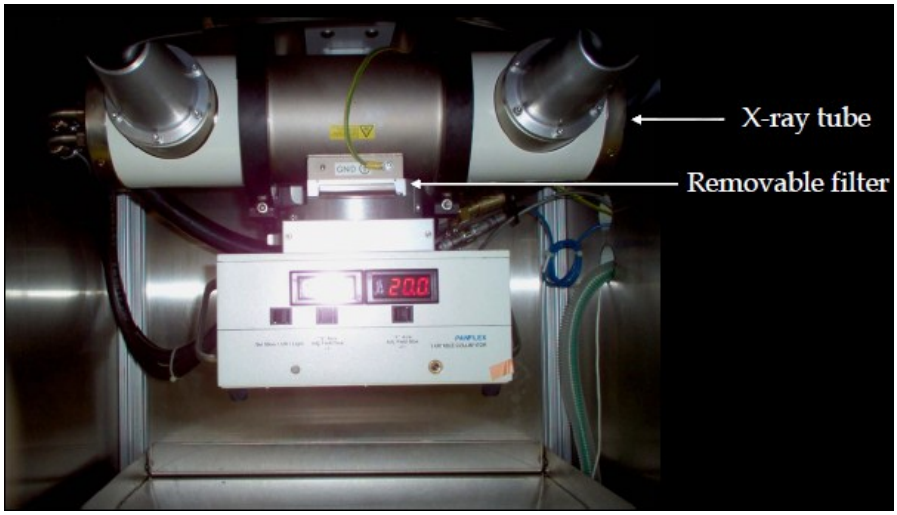

Figure 2.9: The X-ray tube of irradiator

In this project, TLDs were irradiated at approximately100mR exposure level with 60 kVp, 80 kVp and 120 kVp X-ray beams. Radiation parameters for each energy are displayed in Table 2.1.

Table 2.1: X-ray radiation parameters

kVp	Height (cm)	mA	Filter	Time (s)
60	70	1	F4	28
80	70	0.5	F4	20
120	70	0.25	F4	15

2.2.3 Cs-137 Irradiator and Radiation Parameters

A Cs-137 calibration source was used to produce the 662 keV photon beams. The calibration source is located in Klystron Shack Storage #1, Free Electron Laser Laboratory (FELL) at Duke University. Figure 2.10 is an overview of the calibration source. Two sources can be used in this unit: ^{137} Cs Source 1 with a 30 mCi activity and a 8.53 mR/hr dose rate at 1 meter distance on Aug. 01, 2012; ^{137} Cs Source 2 with a 4 Ci activity and a 1031.2 mR/hr dose rate at 1 meter distance on August 01, 2012.

Figure 2.10: The Cs-137 Irradiator

In this project, source 2 was used to irradiate the TLDs. A Plexiglas cover (20cm x 20 cm x 1mm) and base were used to fix the TLDs and ionization chamber for calibration.

Each TLD was placed in the holder in corresponding order. The film was placed behind the Plexiglas frame to determine the field of view. A 0.18cc ionization chamber (10x5-0.18, Radcal, Monrovia, CA) calibrated by University of Wisconsin on August 11 2012 was used to measure the direct exposure of Cs-137 (Figure 2.9).

Figure 2.11: TLDs, film and ionization chamber with Plexiglas frame

TLDs were irradiated using the parameters in Table 2.2. The height in Table 2.2 was the distance between the center level of ionization chamber and table in Figure 2.11.

Table 2.2: Cs-137 Irradiator radiation parameters

Height (inch)	Distance (cm)	Time (s)
10	50	95

2.2.4 Am-Be neutron source and Radiation Parameters

A NIST traceable (NIST Test #273951, Service ID: 44010C) neutron calibration source-Am-Be source was used to calibrate neutron monitors and detectors at Triangle

Universities Nuclear Laboratory (TUNL), Duke University. The emission-rate of the source in August 03, 2007 was 1.233 x 10^6 n/sec. The half-life and average energy of this source are 458 years and 4.4 MeV neutrons, respectively. The source can provide a constant level of neutron flux from the source over approximately 20 years [12]. The Am-Be source also emits 60 keV photons (36% branching ratio) and 14 keV photons (42% branching ratio) [13].

A new Plexiglas frame was fabricated for both TLD-600 and TLD-700 placements (Figure 2.12). The dimension of the frame was 20 cm long, 20 cm wide and 2 cm high. There were 120 square holes with dimension 3.5 mm x 3.5 mm x 1 mm in the middle of one side of the frame for the placement of TLDs.

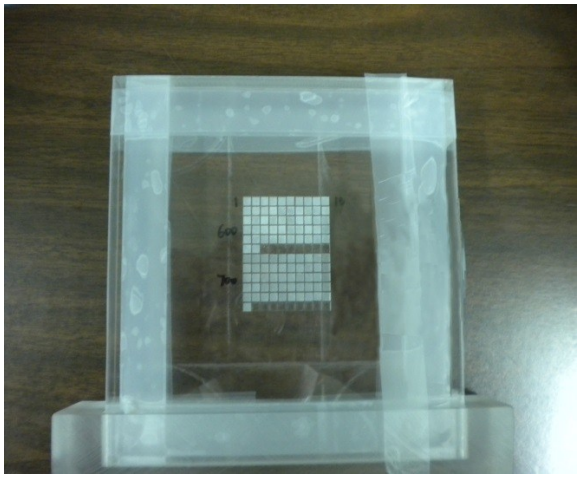

Figure 2.12: TLDs and film badge in Plexiglas frame

Radiation parameters are displayed in Table 2.3

Table 2.3: Am-Be neutron radiation parameters

Distance (cm)	Dose rate (mrem/hr)	Time (min)
50	45.12	133

2.2.5 Individual calibration factor and Average energy correction Factor

An individual calibration factor was defined as:

$$\text{Individual calibration factor} = \frac{\text{The average TLD exposure}}{\text{Individual TLD exposure reading}} \quad \text{2-1}$$

The average exposure of TLD-600 and TLD-700 were calculated respectively from the raw reading.

The average energy correction factor of TLD at photon energy E is defined as

$$\text{Average energy correction Factor} = \frac{\text{Average corrected TLD response}_{\text{E}}}{\text{Average corrected TLD response}_{662\ \text{keV}}} \quad \text{2-2}$$

2.3 Results and Discussion

2.3.1 Physics characterization of TLD-600 and TLD-700 with photon beams

The measured individual calibration factors of TLD-600 and TLD-700 for 60 kVp, 80 kVp, 120 kVp and 662 keV are listed in Appendix C and Appendix D, respectively.

The distribution of calibration factors of TLD-600 and TLD-700 for 60 kVp, 80 kVp, 120 kVp and 662 keV are displayed in Figure 2.13-2.20. From the figures, the TLD response display variances at different energies, therefore individual calibration factors were recommended at each energy level. One possible explanation would be the

electronic configuration for one TLD is different compared to the others'. The electronic configuration in valence band is subdivided into vibrational states of the molecule; thence the energy gaps between the conduction band and valence band are different [1]. This causes the energies of TL photons to be different. It is shown that the distribution of calibration factors of TLD-600 and TLD-700 for all the energies approximately follow the same trend. The reason for this phenomenon is the energy gap between the conduction band and valence band is kept same for the individual TLD with various radiation energies [1].

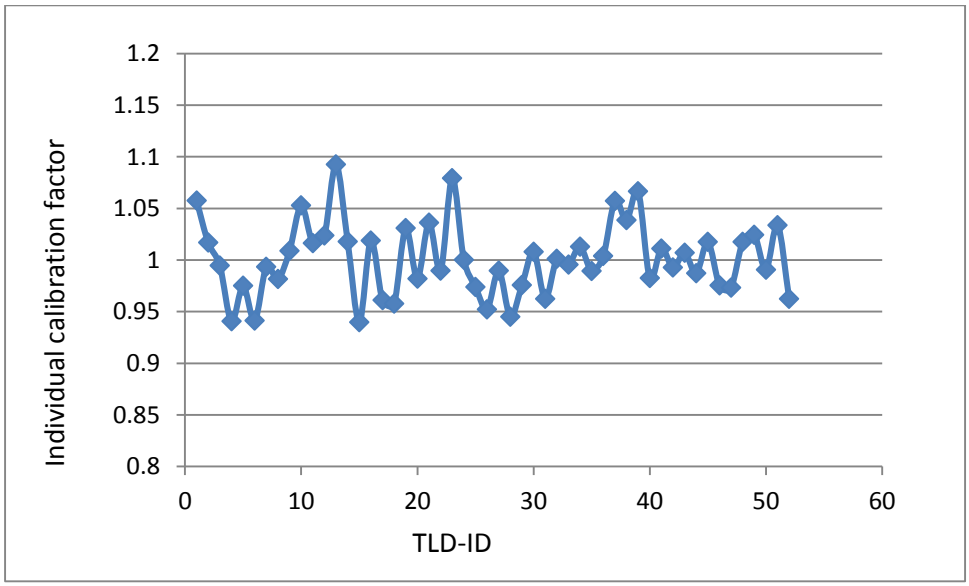

Figure 2.13: The distribution of calibration factors of TLD-600 for 60 kVp photon beams

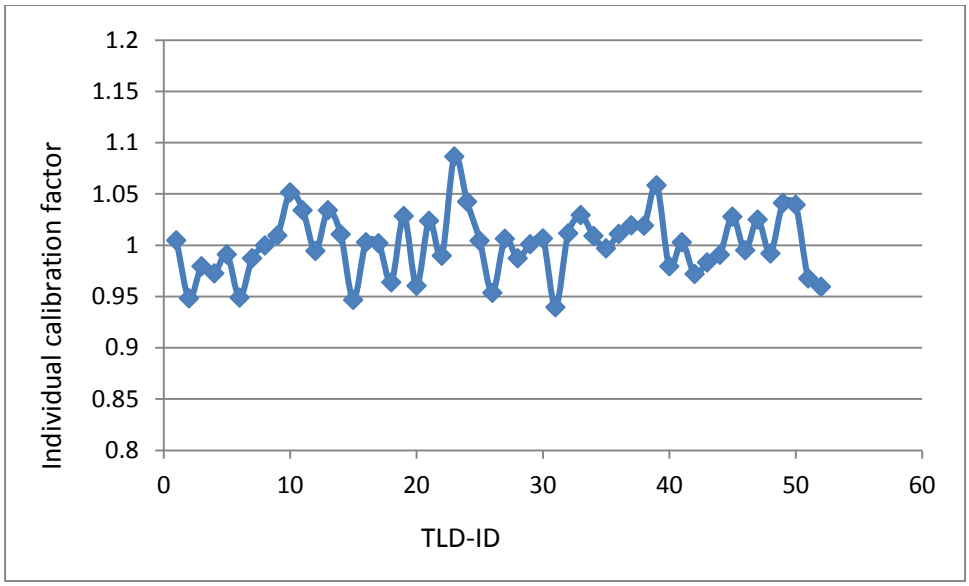

Figure 2.14: The distribution of calibration factors of TLD-600 for 80 kVp photon beams

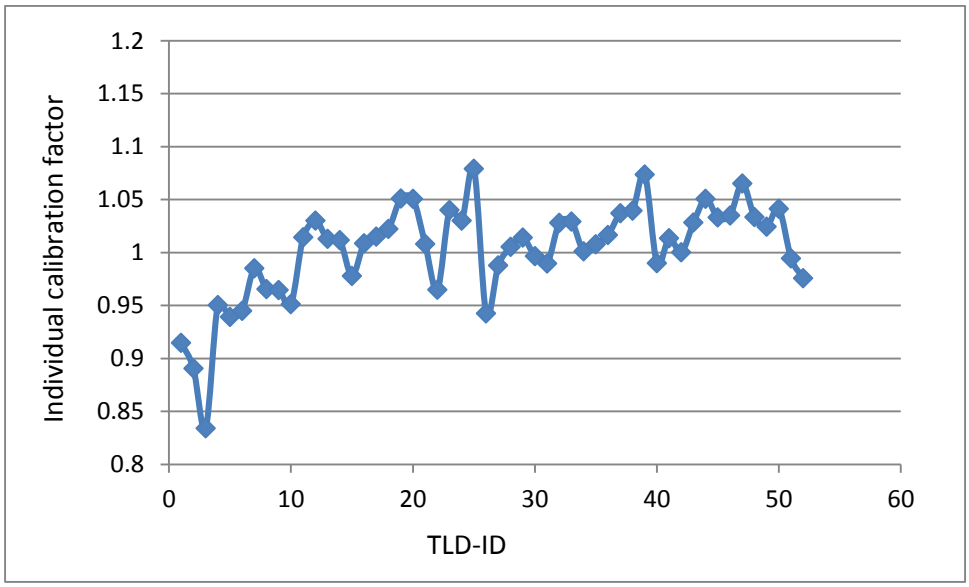

Figure 2.15: The distribution of calibration factors of TLD-600 for 120 kVp photon beams

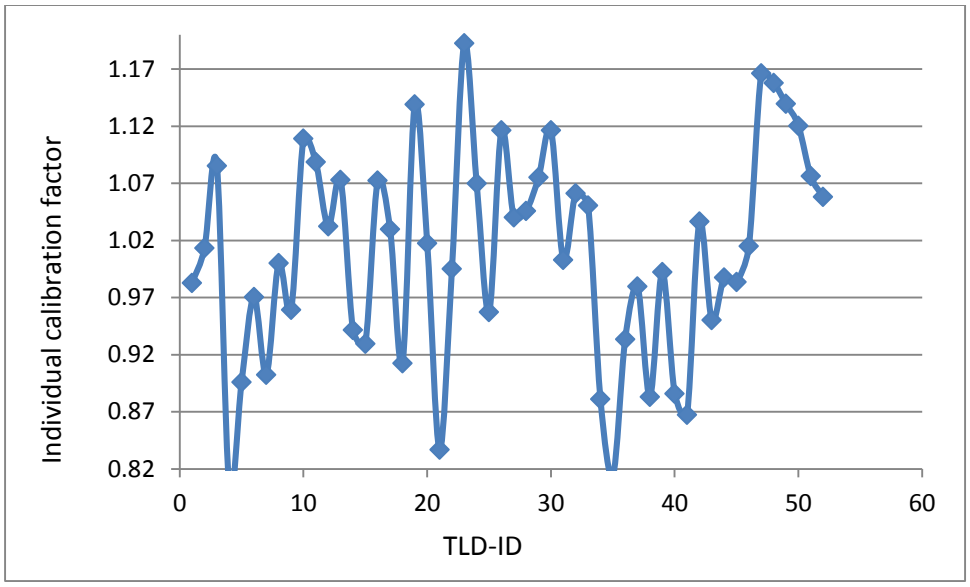

Figure 2.16: The distribution of calibration factors of TLD-600 for 662 keV photon beams

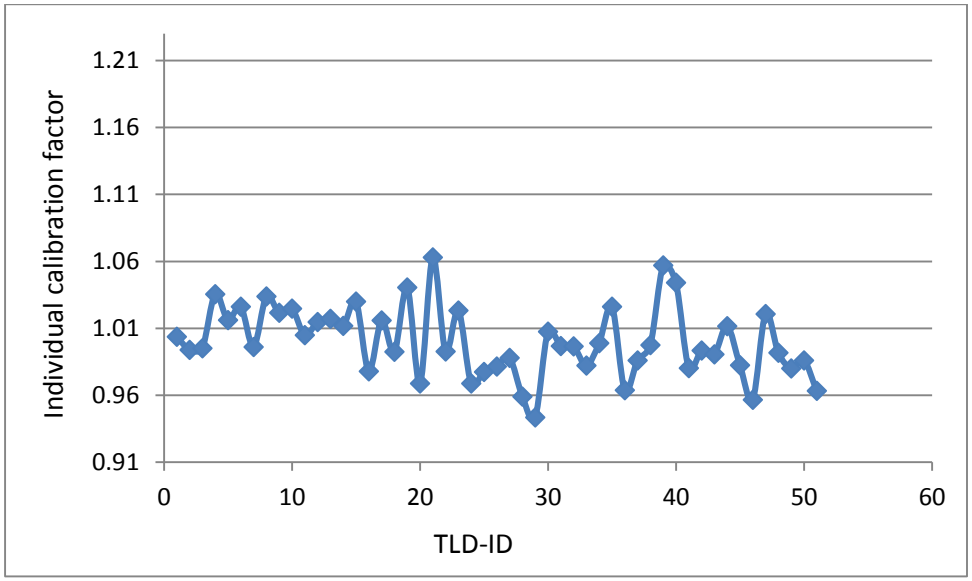

Figure 2.17: The distribution of calibration factors of TLD-700 for 60 kVp photon beams

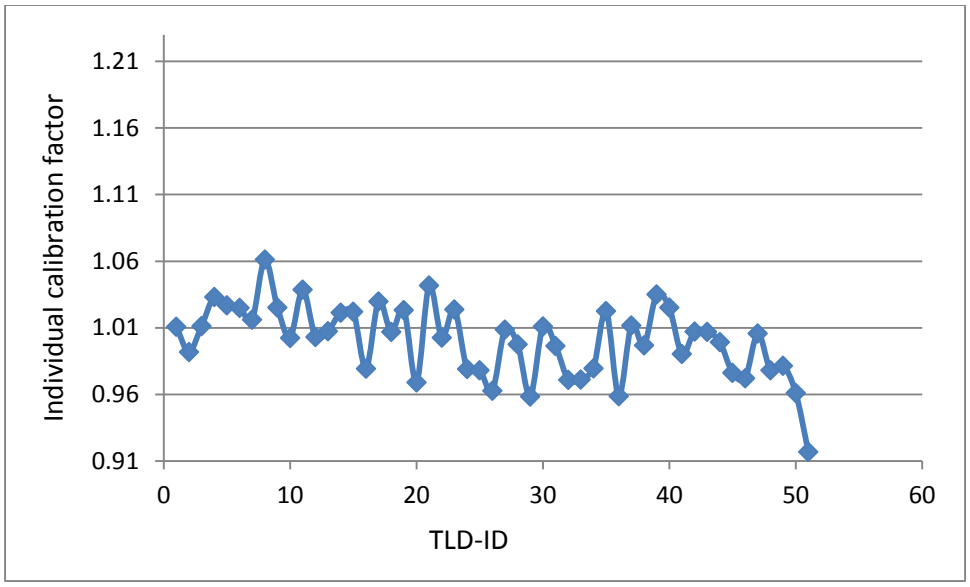

Figure 2.18: The distribution of calibration factors of TLD-700 for 80 kVp photon beams

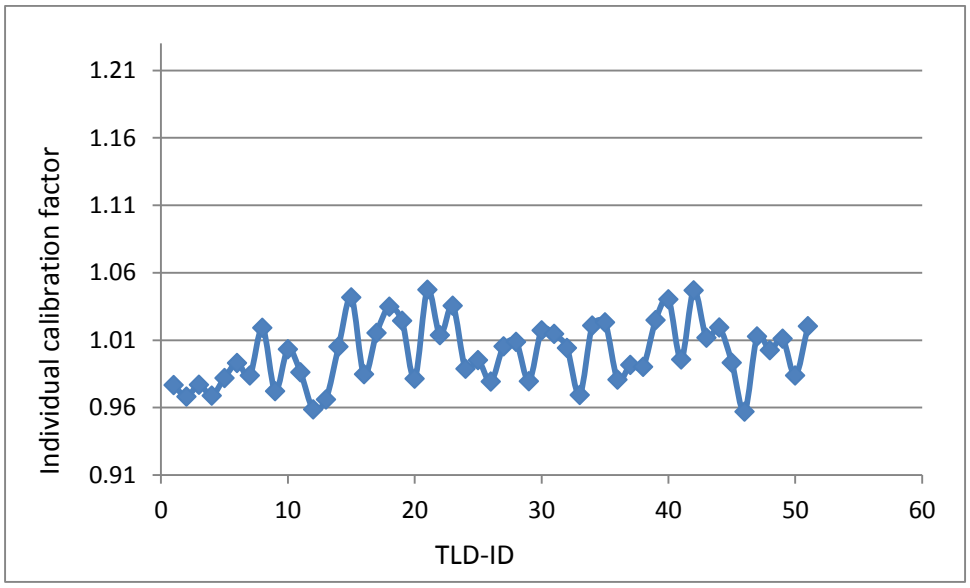

Figure 2.19: The distribution of calibration factors of TLD-700 for 120 kVp photon beams

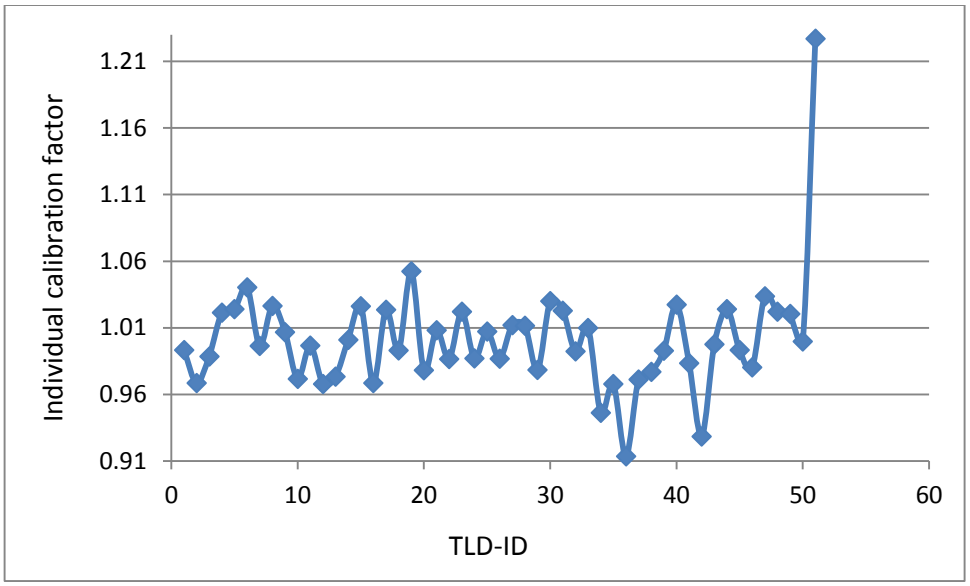

Figure 2.20: The distribution of calibration factors of TLD-700 for 662 keV photon beams

In the figure 2.20, the response of last chip was abnormal compared to others. Each time only 50 chips could be irradiated and read, so last one chip was separated from other 50 chips. If all the chips could be irradiated and read at same time, the results should be similar. It also could be due to the placement, different beam exposure for the two irradiation and difference in manufacture.

The measured average energy correction factors of TLD-600 and TLD-700 for 60 kVp, 80 kVp, 120 kVp and 662 keV with respect to 662 keV are listed in Table 2.4.

Table 2.4: The average energy correction factors of TLD-600 and TLD-700 for 60 kVp, 80 kVp, 120 kVp and 662 keV to 662 keV photon beams

Energy	TLD-700	TLD-600
60 kVp	1.0373	1.2223
80 kVp	0.9766	1.1013
120 kVp	0.8853	1.0299
662 keV	1	1

The average energy correction factors for these four energy photon beam ranged from 0.817 to 0.999 for TLD-600 and from 0.8 to 0.937 for TLD-700 would explain the energy dependence TLDs have.

At the increased energy, the average energy correction factors decreased for TLD-600 and TLD-700. A potential possibility would be due to more and more electrons in higher vibrational ground states are free by ionizing process that only the electrons in lowest vibrational state is left to be excited. Another possible reason would be the dominance of the photoelectric effect for lower energy radiation that would produces a larger thermoluminescent yield.

Table 2.5: The average response of TLD-600 and TLD-700 for 60 kVp, 80 kVp, 120 kVp and 662 keV to 662 keV photon beams

Energy	TLD-700 (nc/mR)	STDEV (nc/mR)	TLD-600 (nc/mR)	STDEV (nc/mR)
60 kVp	0.0937	0.0035	0.0999	0.0024
80 kVp	0.0882	0.0028	0.0900	0.0024
120 kVp	0.0800	0.0041	0.0842	0.0019
662 keV	0.0904	0.0079	0.0817	0.0035

The measured average response of TLD-600 and TLD-700 for 60 kVp, 80 kVp, 120 kVp and 662 keV are listed in Table 2.5. It can be seen that the average response of TLD-600 and TLD-700 are different for each energy level. The average response of TLD-600 is larger than that of TLD-700 for each energy level except for the 662 keV energy photon beam. The possible reason would be due to the energy gaps between the valence band and conduction band for TLD-600 is larger than that of TLD-700. Another possibility would be the excited energy from the traps for TLD-700 is closer to the edge of the band

gap which the electron could return to the conduction band easier during the 24 hours prior to reading.

Figure 2.21 displays the response for different energies of LiF based TLD relative to Cs-137 and J E Ngaile et al. characterized the LiF TLD-100s using 40, 60, 80, 100, 120 and 150kVp X-ray [14], The results in this study is similar to J E Ngaile's result.

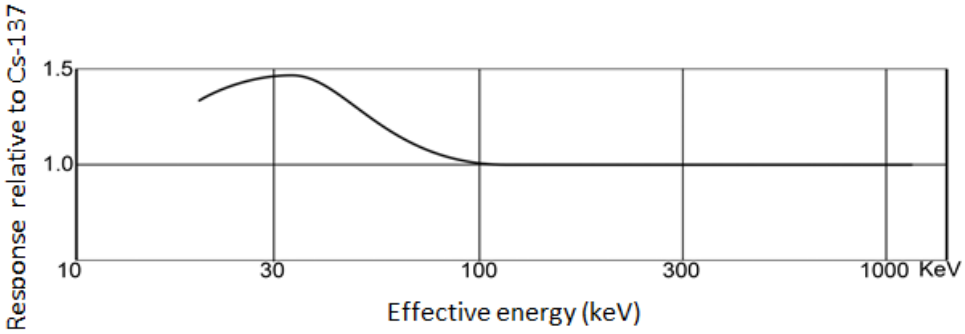

Figure 2.21: The response of LiF based TLDs relative to Cs-137

2.3.2 Physics characterization of TLD-600 and TLD-700 with neutron beams

The measured individual calibration factors of TLD-600 for Am-Be neutron beams are listed in Appendix E.

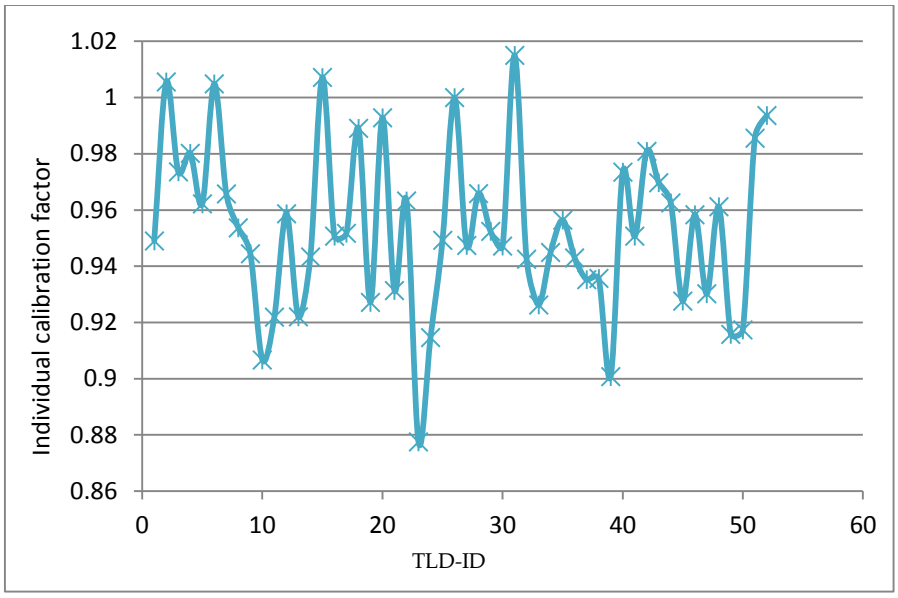

Figure 2.22: The distribution calibration factors of TLD-600 for Am-Be neutron beams

The distribution of calibration factors of the 51 TLD-600 chips for Am-Be neutron beams are displayed in Figure 2.22.

The measured individual calibration factors of TLD-700 for Am-Be neutron beams are listed in Appendix F.

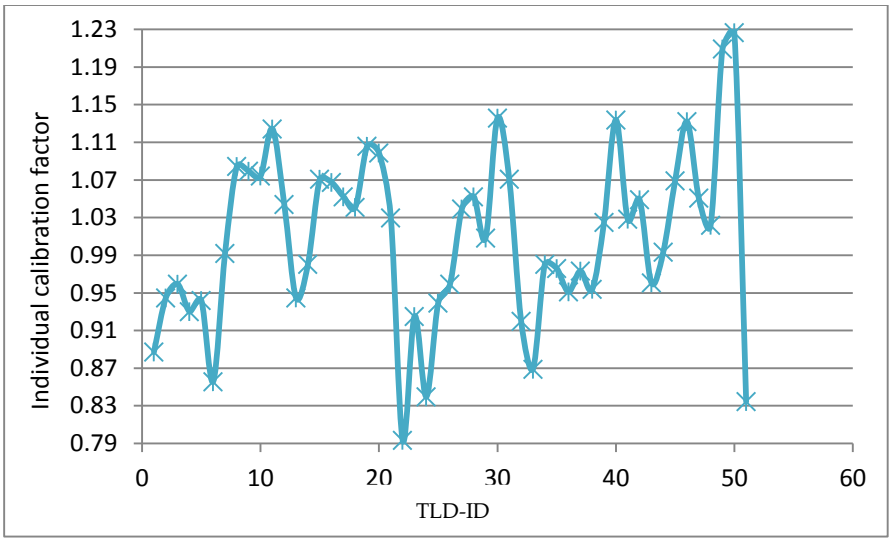

Figure 2.23: The distribution calibration factors of TLD-700 for Am-Be neutron beams

The distribution of calibration factors of TLD-700 for Am-Be neutron beams are displayed in Figure 2.23. Because the TLD-700 can only measure photon beam and the photon energies include several energy levels, the individual response pattern of calibration factors for the Am-Be neutron beams is completely different from that for 60 kVp, 80 kVp, 120 kVp and 662 keV photon beams by comparing Figure 2.23 to Figure 2.17- 2.20.

During the analysis, it was noted some TLD reading were abnormally higher than the others. After exposing 60 kVp X-ray beams, TLD-600 were read firstly. It was found that the response of the initial 5 chips of TLD-600 after warming up the machine was much greater than others. It was possible that the reader was not fully warmed it up and has been recommended that 30 chips of TLD-100s were read prior to reading any exposed TLDs. After the dummy chips were read, the TLD-600 and TLD-700 results

came out consistent without high variation. Therefore, after this finding, the TLDs were re-exposed to various energies and followed this procedure to obtain more accurate results.

2.3.3 General discussion

As the energy of photon beams approaches 662Kev, the average energy correction factor approaches one. For all energy after 662 Kev, the energy correction factor is one. The energy of the photon beams in TUNL ranges from 2 to 60 MeV. Therefore, for TUNL environmental monitoring, it is suggested that individual calibration factors from the 662 keV photon beams is applied to TLD-700. For TLD-600, the individual calibration factors only obtained from 4.4 MeV neutron beams. The energy of neutron beam produced in the TUNL ranges from 8 to 14 MeV. Therefore, to achieve the goal of TUNL environmental monitoring, the next step is to study the individual various responses and the energy responses of TLD-600 by irradiating the TLD-600 using 8-14 MeV neutron beams.

2.4 Conclusion

We have measured individual calibration factors and the average energy correction factors for photon beams and Am-Be neutron beams. Our results will be used in the future experiments and measurements with TLD-600 and TLD-700.

3. Acceptance testing of new X-RAD 160 Biological X-Ray Irradiator

3.1 Introduction

A new X-RAD 160 Biological X-ray irradiator (Figure 3.1) was purchased from Precision X-ray Inc. (North Branford, CT) and installed in Levine Science Research Center (LSRC) at Duke University. The general application of this machine is for cellular radiobiology research, with the specific application being cell and molecular biology experiments.

This will describes the acceptance test procedures employed for the irradiator. Acceptance testing is extremely important, because it ensures that all researchers can work safely while doing experiments with the machine and that the irradiation specifications are sufficient for quality research.

For diagnostic or therapeutic X-ray equipment, well defined protocol or procedures are available for acceptance testing, e.g. AAPM Report No. 14 [15].

For this project, the specifications were not available and therefore the components or the acceptance in this study were determined based on the actual application of this system, e.g. leakage radiation survey, the tests of tube current linearity (linearity of mA), kVp accuracy, field size measurements, beam quality, exposure consistency and field uniformity, etc.

The leakage radiation survey can check if leakage radiation is present. The test of linearity of mA is measure the radiation exposure at various mA to check whether the

machine can produce a constant radiation output, linearity with tube current is expected [15]. The kVp accuracy is most critical because a small error of kVp would have a greater effect on the dosimetric experiments than any other parameters [15]. The field size is measured by determining the effective radiation field size at a certain distance between the radiation source and detector [15]. The test of beam quality is to measure the half value layer (HVL), which means to test the penetrability of the beam when no energy spectrum of x-ray beam is known [15]. Exposure consistency tests whether the radiation exposure is precisely the same if any or all of the radiation parameters are changed and then returned to the previous value [15]. The test of field uniformity is to measure whether the intensity of the beam in a horizontal plane is uniform [15].

Mohaupt et al performed the acceptance testing using a 60 kVp X-ray irradiator [16]. This acceptance testing of this project applied some methods from Mohaupt's study.

Figure 3.1: One example of biological X-Ray irradiator

3.2 Material and Methods

3.2.1 X-RAD 160 Biological X-Ray Irradiator

The X-ray irradiator includes of an X-ray tube, a cooling unit and a shielded cabinet. It can be operated at voltages of 5-160 kVp in 0.1 kVp increments and currents of 0.1-18 mA in increments of 0.01 mA [17]. The exposure time can be set from 1 to 9999 seconds [17]. Water cooling allows the tube to be operated continuously. A 45 degree angle in the tungsten target was used to minimize anode heel effects [17]. An inherent filtration of 0.8mm of beryllium (Be) was used for beam hardening [17].

The control panel is a multi-user, password protected touchable graphical interface. It can show and save all exposure parameters and data can be transportable. The programmable exposure settings allow for fast and repeated exposure setup [17].

The dimensions of the cabinet are 42 cm x 42.75 cm x 55 cm (Figure 3.2). The shielded cabinet consists of an adjustable specimen shelf ranged from 0-48 cm from the source to the shelf, sample viewing window and beam hardening filter station.

Aluminum (Al) filters were added the exit port of the Be window to increase the effective energy of the X-ray beam by removing many of the low-energy X -rays. A filter of 2 mm thick Al was used for all dosimetric measurements [17].

Figure 3.2: The cabinet of the irradiator

A safety light is turned on at the head of the irradiator when the machine is on to alert occupants in the room that x-ray are being produced. When the cabinet door is open during X-ray generation, the beam is turned off automatically by an interlock mechanism [17].

3.2.2 Components

3.2.2.1 Acceptance testing on September 21, 2012

3.2.2.1.1 Leakage Radiation Safety Survey

When the irradiator was on at maximum power (160 kVp, 18mA, 200s) , the Radiation surveys were taken at the exterior surface of the irradiator using the Victoreen 451 survey meter (Serial # 3516 Cal Due: 11/01/2011). The exposure rate was recorded in μR/hr.

3.2.2.1.2 Beam Quality

The distance between the detector and the source was 40 cm. The Half Value Layer (HVL) was measured without filter at several kVps and 1 mA.

3.2.2.1.3 KVp accuracy

The distance between the source and the Piranha, the time and the tube current maintained at 40 cm, 15s and 10mA without filter, respectively. The kVp was recorded from 50 kVp to 150 kVp in 10 kVp incensement using the Piranha. Then the irradiator kVp was compared to the kVp measure by the Piranha to check the kVp accuracy.

3.2.2.1.4 Linearity of mA

The distance between the source and the chamber was 40 cm without filter. The peak tube voltage and time were maintained at 160 kVp and 15 Secs. The exposure of the irradiator was read in R by the ionization chamber as the tube current varied from 2 mA to 18mA.

3.2.2.1.5 Exposure Consistency

The distance between the source and the ionization chamber was 40 cm without filter. The peak tube voltage, tube current, and time was maintained at 160 kVp, 18 mA, and 20s, respectively. A series of three exposures of the irradiator of at the same setting was read in R by the ionization chamber.

3.2.2.1.6 Field Size Measurements

The peak tube voltage, tube current, and time was set to 160 kVp, 10 mA, and 15s, respectively. The effective field size at a distance 40 cm between the source and the film with filter 1 was measured using film.

3.2.2.1.7 Beam Uniformity in the X-Y Plane

The exposure of the irradiator recorded in R was measured at a 40cm distance between the source and shelf in the horizontal plane with the ionization chamber and without a filter. The peak tube voltage, tube current, and time was set to 160 kVp, 18 mA, and 15s, respectively. Along the geometrical center, the output was measured toward the x and y directions.

3.2.2.1.8 Inverse Square Measurements

The peak tube voltage, tube current and time was set to 160 kVp, 1 mA, and 30s, respectively. The exposure of the irradiator was read in R by the ionization chamber with increasing distance between the source and shelf was measured without filtration.

3.2.2.2 Acceptance testing on November 18, 2012

3.2.2.2.1 Beam Quality

The distance between the detector and the source was 40 cm. The Half Value Layer (HVL) was measured with F1 filter at several tube currents and tube voltages.

3.2.2.2.2 KVp accuracy

The distance between the source and the Piranha, the time and the tube current maintained at 40 cm15s and 1mA with F1 filter, respectively [21]. The kVp was recorded after one shot from35 kVp to 150 kVp using the Piranha. The actual kVp was compared to the kVp recorded by the Piranha to check the kVp accuracy.

3.2.2.2.3 Variation of kVp

The distance between the source and the ionization chamber was 40 cm with filter 1 in-place. The time and tube current were set at 30s and 18mA, respectively. The exposure of the irradiator was read in R by the ionization chamber with the varying tube voltages.

3.2.2.2.4 Linearity of mA

The distance between the source and the chamber was 40 cm with F1 filter in-place. The peak tube voltage and time were maintained at 160 kVp and 30s. The exposure of the irradiator was read in R by the ionization chamber as the tube current varied from 1 mA to 18mA.

3.2.2.2.5 Beam Uniformity in the X-Y Plane

The exposure of the irradiator recorded in R was measured at a 40cm distance between the source and shelf in the horizontal plane with the ionization chamber and F1

filter in-place. The peak tube voltage, tube current, and time was set to 160 kVp, 18 mA, and 30s, respectively. Along the geometrical center, the output was measured toward the x and y directions. Film was used to verify the uniformity of the irradiator.

3.2.2.2.6 Inverse Square Measurements

The peak tube voltage, tube current and time was set to 160 kVp, 18 mA, and 30s, respectively. The exposure of the irradiator was read in R by the ionization chamber with increasing distance between the source and shelf was measured without filtration.

3.3 Results and Discussion

There were two tests and maintenance tasks in between the two dates.

3.3.1 Acceptance testing on September 21, 2012

3.3.1.1 Leakage Radiation Safety Survey

The results showed there was no additional radiation exposure due to leakage of the beam, and all exposure readings were found to be at background level. The radiation survey data is in Appendix G.

3.3.1.2 Beam Quality

Table 3.1 shows beam quality data. As the peak tube voltage increases, the HVL increases.

Table 3.1: Parameters of Beam Quality

SID(cm)	kVp	mA	Filter	TF(mm)	HVL(mm)
40	50	1	None	1	1.07
40	60	1	None	1	1.28
40	70	1	None	1	1.50
40	80	1	None	1	1.76
40	90	1	None	1	2.06
40	100	1	None	1	2.35
40	110	1	None	1	2.67
40	120	1	None	1	3.00
40	130	1	None	1	3.42
40	140	1	None	1	3.81
40	150	1	None	1	-

3.3.1.3 KVp accuracy

Table 3.2 shows the reading of Piranha with the varying tube voltage. The differences between the kVp of the irradiator and the kVp of reading ranged from 0.0667% to 1.860%. The error in kVp was found to be less than 2% for all kVp settings.

Table 3.2: The kVp accuracy

kVp	Reading-kVp	Difference
50	50.93	1.9%
60	60.89	1.5%
70	70.69	0.99%
80	80.82	1.0%
90	91.29	1.4%
100	100.8	0.80%
110	110.4	0.36%
120	119.8	0.17%
130	131.1	0.85%
140	141.1	0.786%
150	150.1	0.0667%

3.3.1.4 Linearity of mA

Figure 3.3 displays the response of the ionization chamber as the tube current varied. The results show the linearity of the X-ray output fulfills the agreement over the entire range of tube current.

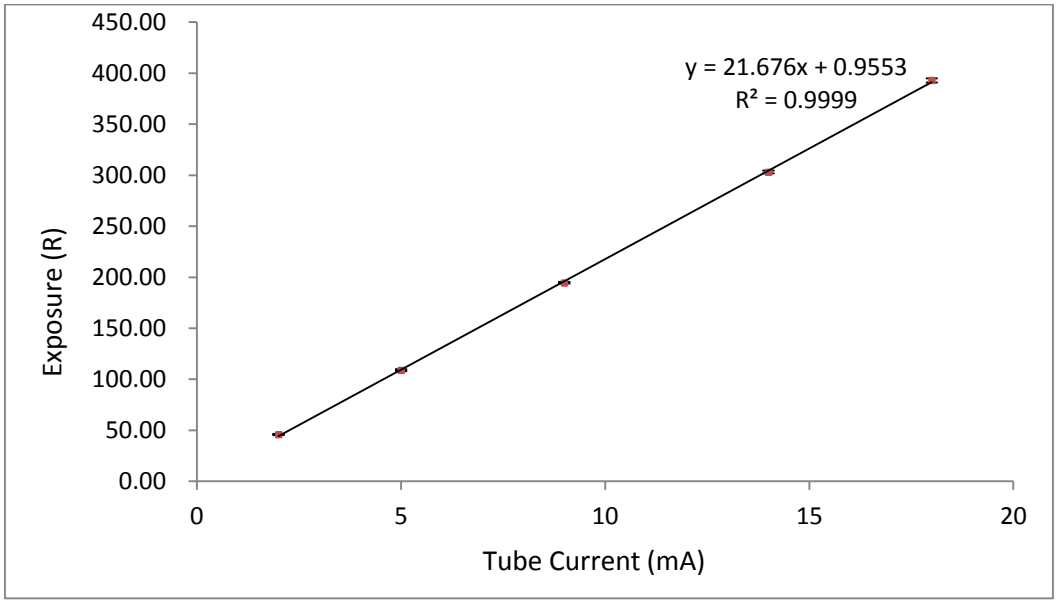

Figure 3.3: Linearity of X-ray output with tube current

3.3.1.5 Exposure Consistency

Table 3.3 shows response of the ionization chamber of a series of three exposures at the same setting. The differences between the individual exposure and the average exposure ranged from -0.18 to 0.10%.

Table 3.3 Exposure Consistency

No.	Exposure (R)	Difference From Average
1	529.61	0.10%
2	529.51	0.08%
3	528.17	0.18%
Average	529.09	
STDEV	0.8059	

3.3.1.6 Field Size Measurements

Figure 3.4 displays the effective field size, which was a circular with a 12 cm diameter.

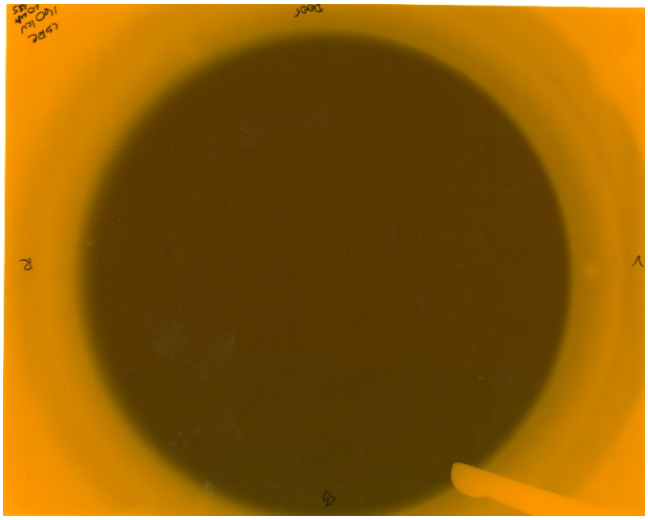

Figure 3.4: The field size of the irradiator at 40 cm

3.3.1.7 Beam Uniformity in the X-Y Plane

Figure 3.5 and 3.6 display exposure distribution along the field of view in x-direction and y-direction, respectively. The geometrical center of the X-ray beam was the same as the center of the field.

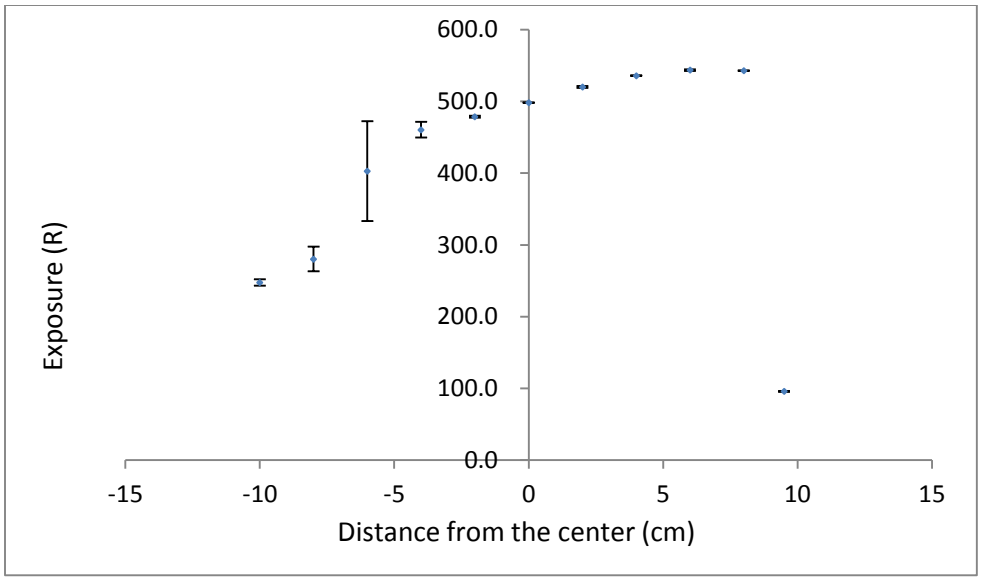

Figure 3.5: Field uniformity measurement at x-direction

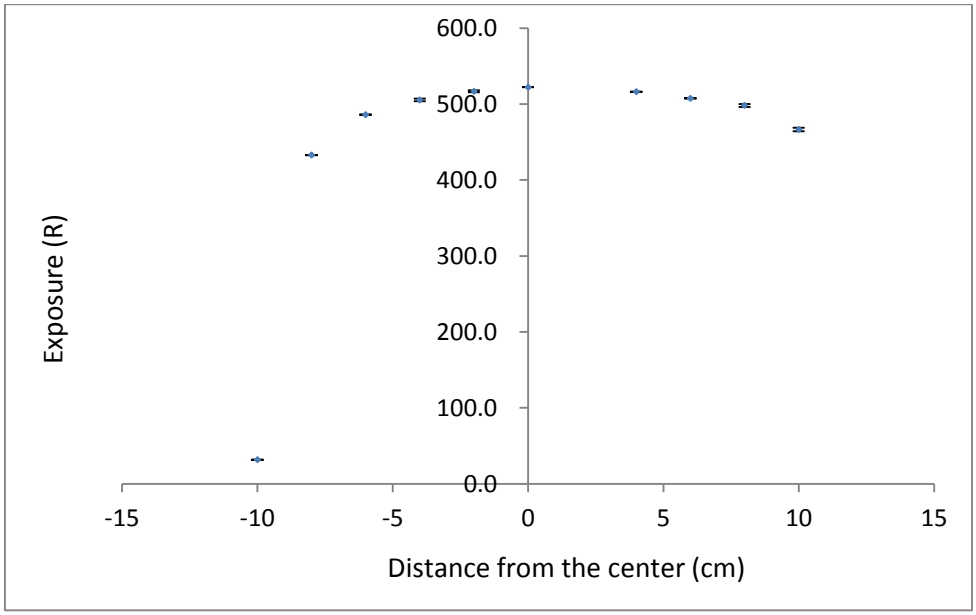

Figure 3.6: Field uniformity measurement at y direction

Figure 3.5 shows that the x-axis reading was not uniform. Since the measured exposure along the X-axis is from speaking in very non-uniform and the exposure greatly decreases going in the left direction. This indicates that un-corrected anode heel

effect was present. Consequently, for any dosimetric validation we could not use this machine because common 6-well cell plates cannot be under uniform exposure. The unit failed this component of the acceptance testing, and was returned to the vendor for modifications. Recommendations have been made by staff and students of the DRDL to the vendor about the potential design flaw of the x-ray tube positioning.

3.3.1.8 Inverse Square Measurements

Figure 3.7 shows the relationship between the source-detector distance and measured exposure. The data in Figure 3.9 were fitted with a power function, as shown.

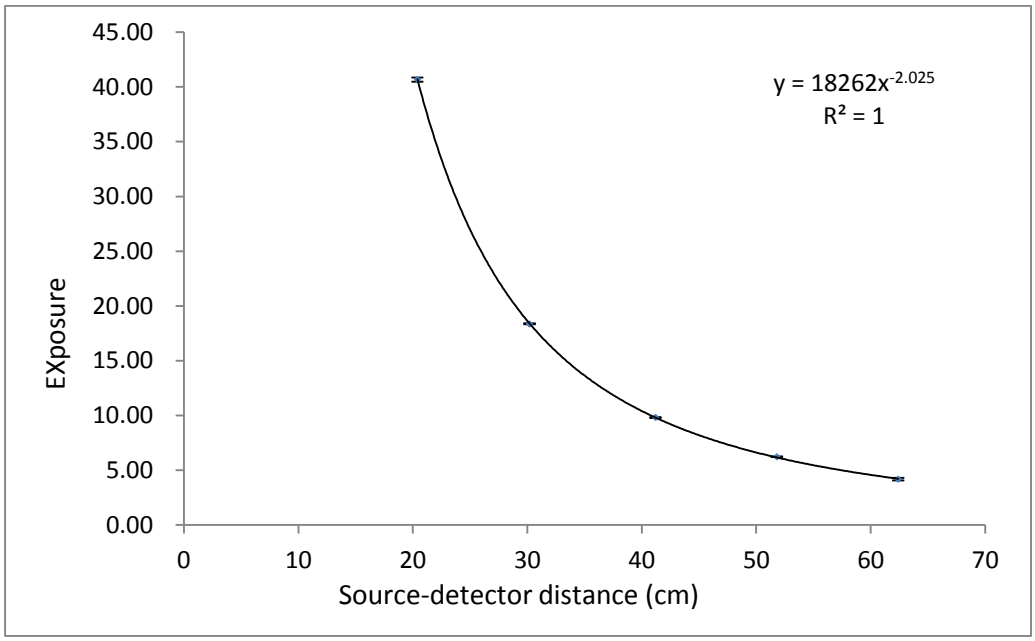

Figure 3.7: Radiation output measurements of Inverse Square Law

3.3.2 Acceptance testing on November 18, 2012 after remodeling

The X-ray tube was returned to the manufacturer, who reconfigured the beam by tilting the X-ray tube which is shown is Figure 3.8. The holder of the X-ray tube was to

remove the gap between X-ray tube and base. Once the tube was returned, another round of acceptance testing was performed on November 18, 2012.

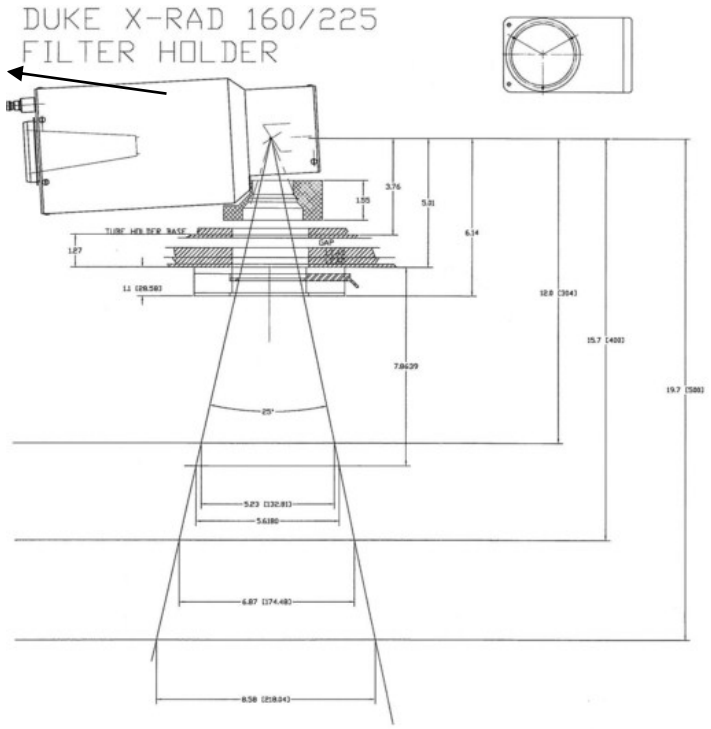

Figure 3.8: The scheme of the X-ray tube after fixing

3.3.2.1 Beam Quality

Table 3.4 shows beam quality at several kVps. As the peak tube voltage increases, the HVL increases.

Table 3.4: Parameters of Beam Quality

SID(cm)	kVp	mA	Filter	TF (mm)	HVL (mm)
40	35	1	F1	-	-
40	50	1	F1	1.8	1.46
40	70	1	F1	1.6	1.86
40	90	1	F1	1.4	2.36
40	120	1	F1	1.4	3.40
40	140	1	F1	1.2	4.02
40	150	1	F1	1.2	-

3.3.2.2 KVp accuracy

Table 3.5 shows the reading of Piranha with the varying tube voltage. The differences between the kVp of the irradiator and the kVp of reading ranged from 0.43% to 2.1%. The error in kVp was found to be less than 2.1% for all kVp settings.

Table 3.5: The kVp accuracy

kVp	Reading kVp	Difference
35	35.74	2.1%
50	50.81	1.6%
70	70.3	0.43%
90	90.85	0.94%
120	119.1	0.75%
140	141.6	1.1%
150	151.1	0.73%

3.3.2.3 Variation of kVp

Figure 3.9 shows the response of the ionization chamber with the varying tube voltage. Power function curves were used to compare the data in Figure 3.11, as shown. The power function correlation coefficient was greater than 0.998.

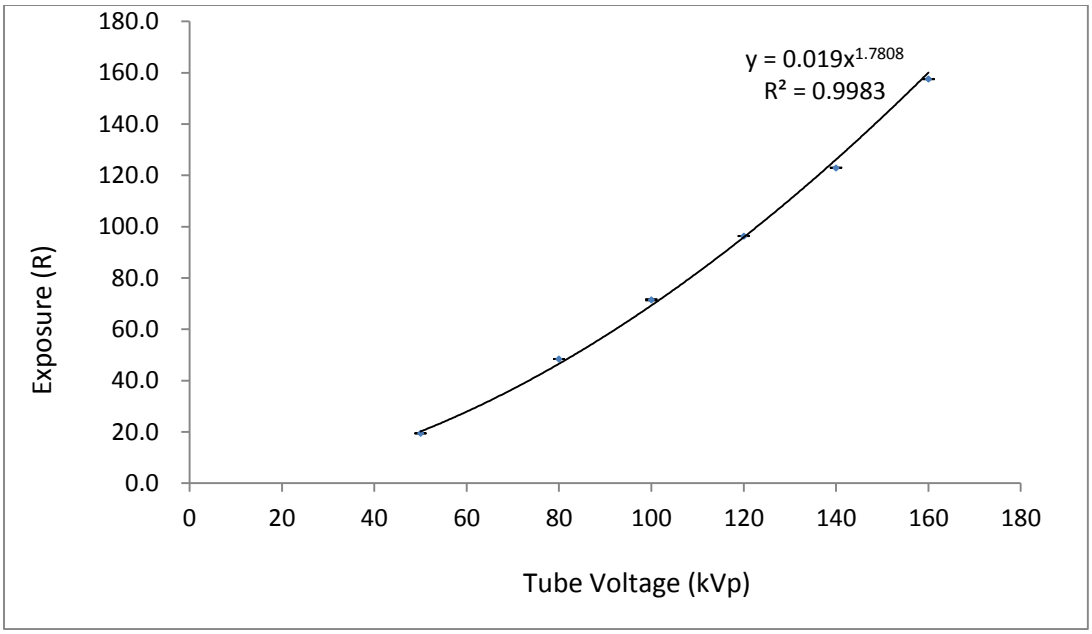

Figure 3.9: X-ray output as a function of tube voltage

3.3.2.4 Linearity of mA

Figure 3.10 displays the response of the ionization chamber as the tube current varied. The results show the linearity of the X-ray output fulfills the agreement over the entire range of tube current.

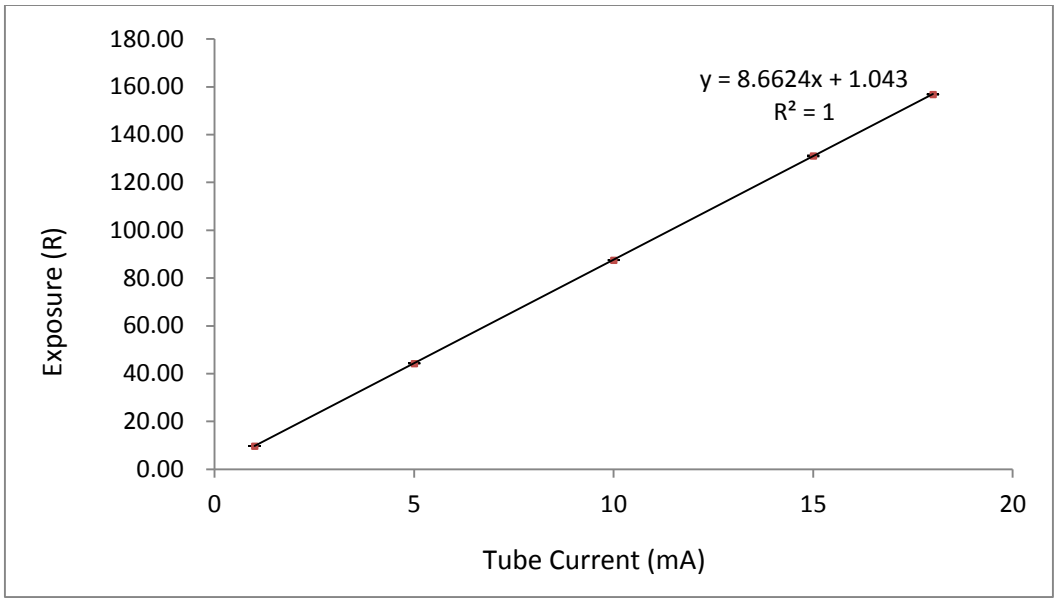

Figure 3.10: Linearity of X-ray output with tube current

3.3.2.5 Beam Uniformity in the X-Y Plane

Figure 3.11 and 3.12 display exposure distribution along the field of view in x-direction and y-direction, respectively. The geometrical center of the X-ray beam was same as the center of the field.

Figure 3.13, 3.14 and 3.15 were obtained from the film. Compared to Figure 3.5 and 3.6 the new data shows that the beams were uniform.

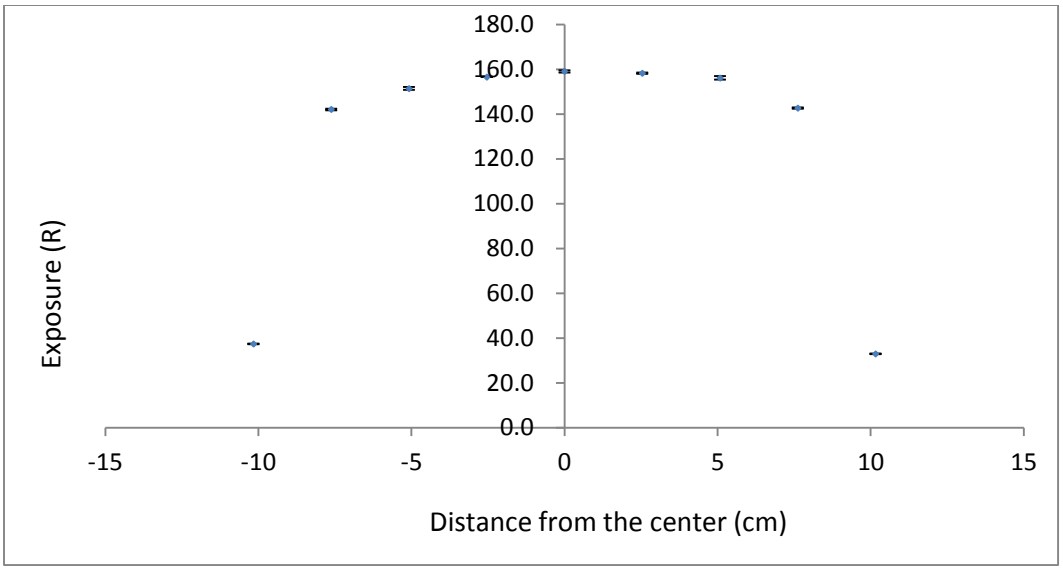

Figure 3.11: Field uniformity measurement in x-direction

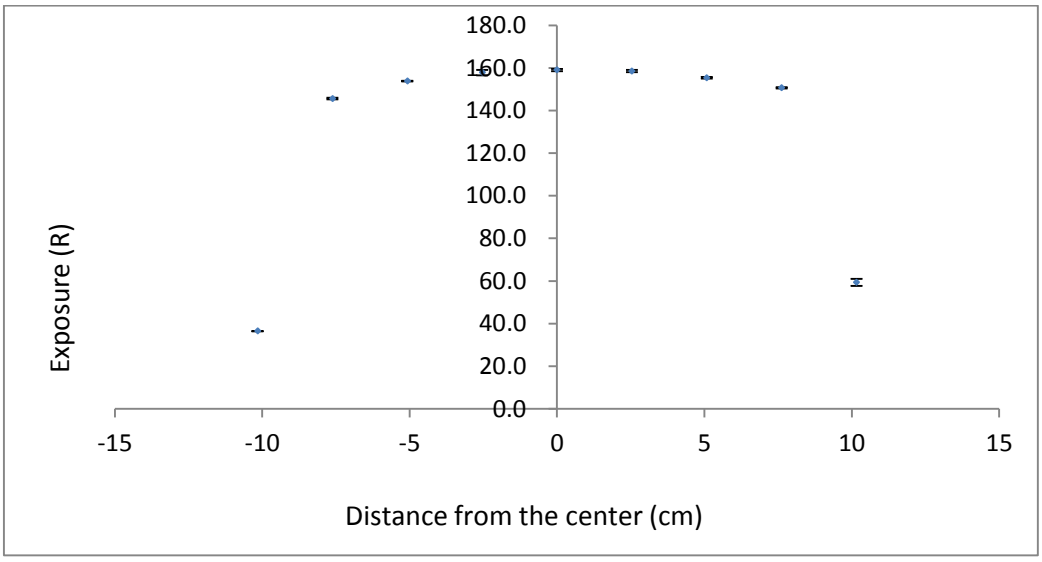

Figure 3.12 Field uniformity measurements in y-direction

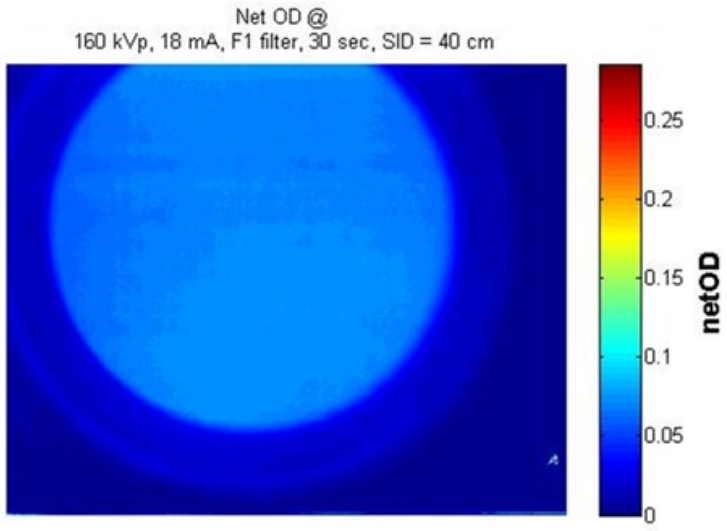

Figure 3.13: Film of field uniformity measurement

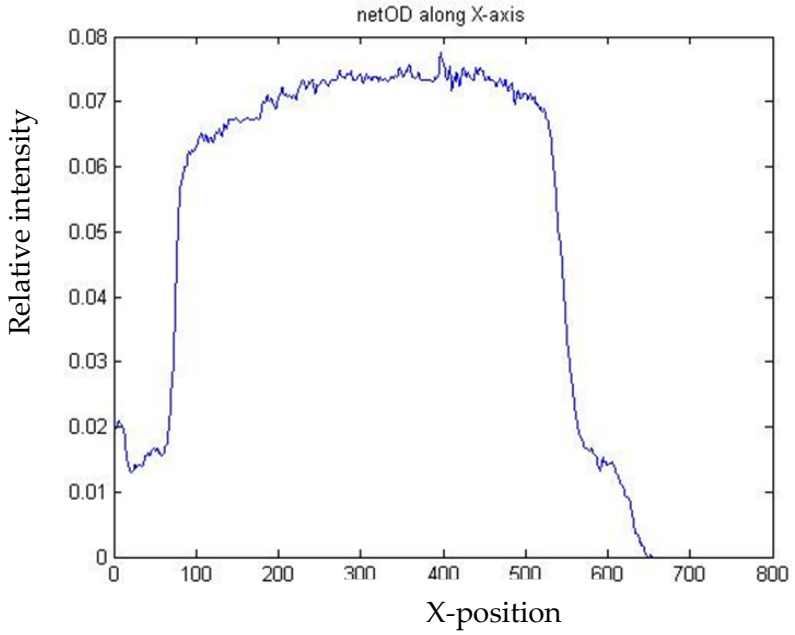

Figure 3.14: Line Profile from uniformity measurement in x-direction

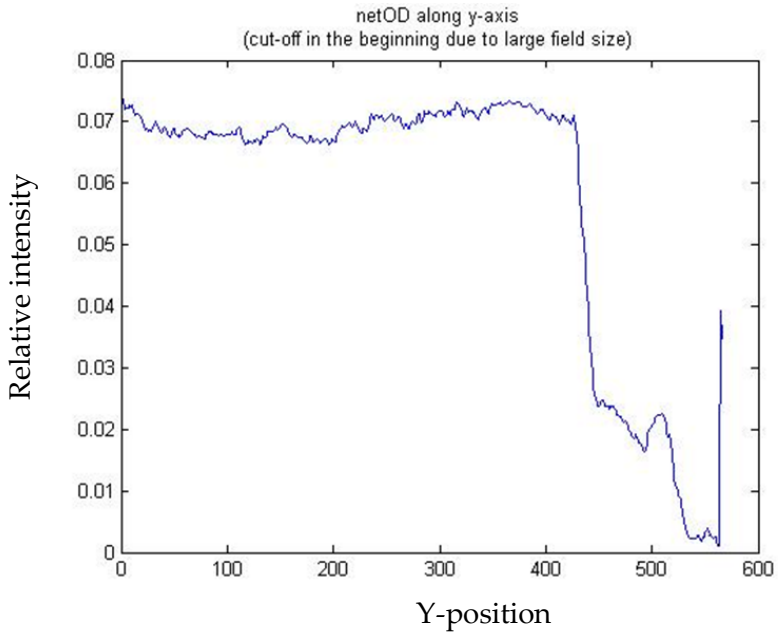

Figure 3.15: Line Profile from uniformity measurement in y-direction

3.3.2.6 Inverse Square Measurements

Figure 3.16 shows the relationship between the source-detector distance and measured output of the ionization chamber. The data in Figure 3.18 were fitted with a power function, as shown.

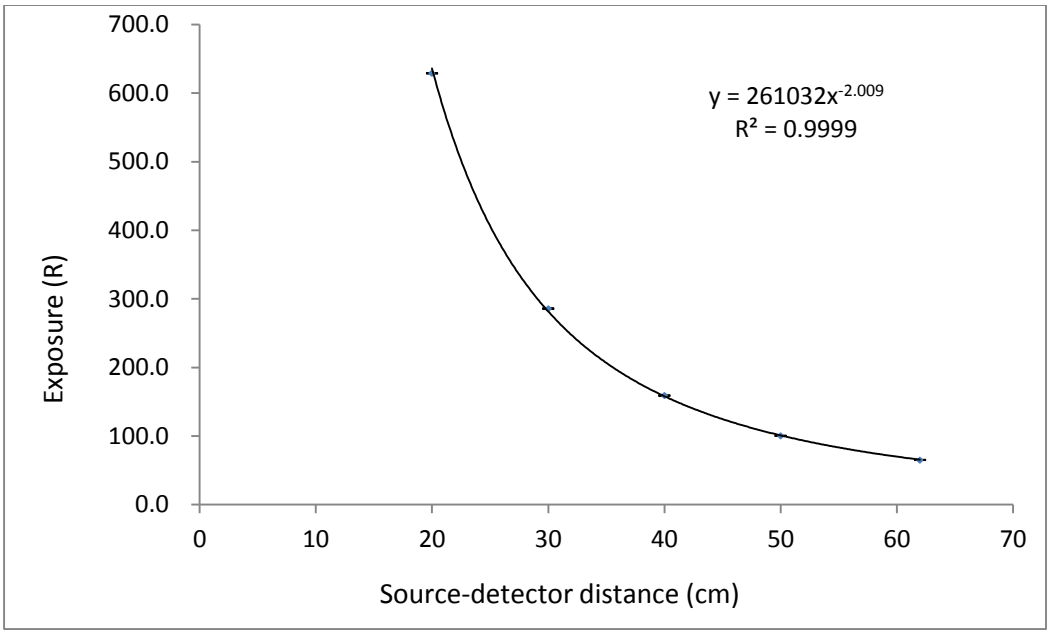

Figure 3.16: Radiation output measurements of Inverse Square Law

3.3.3 General discussion

The purpose of the acceptance testing was completed by these tests, but several limitations were available in the testing: (1) in the measurement of uniformity, the exposure was measured in only two axes. The exposure was also measured in the four quadrants. But the anode heel effect was the most important problem and was found and addressed. (2) In the test of kVp accuracy, due to the Piranha's limited measuring range in kVp (35 – 155 kVp)and machine, only several kVps was measured. But the numbers of kVps were enough to check the kVp accuracy.

The acceptance testing was the first round of benchmark that various geometric setups for cellular radiological research would be performed with the data from the acceptance testing. The passing of the acceptance is only the initial part of our quality assurance (QA) program, routine maintenance and QA measurements are required in the future. In addition, the training of operators is equally important to ensure the correct operation procedures are followed.

3.4 *Conclusion*

The first round of acceptance testing performed on September 21, 2012 failed because the measured exposure along the X-axis was significantly non-uniform. After the X-ray tube was returned to the manufacturer, the beam was reconfigured by tilting the X-ray tube and another round of acceptance testing was performed on December 18, 2012. The results of second round of acceptance testing showed there was no radiation hazard for the researcher surrounding the new X-RAD 160 Biological X-Ray Irradiator and the machine had a uniform and consistent beam. The data established baseline values for the parameters for future QA program. In the following research, routine maintenance and quality QA are required.

Appendix A

Table Appendix: The TTP for TLD-600 and TLD-700 [10]

TLD	*Preheat Temp (0C)*	*Preheat Time (Sec.)*	*Acquisition Rate (0C/Sec.)*	*Acquisition Max Temp (0C)*	*Acquisition Time (Sec.)*	*Anneal Temp (0C)*	*Anneal Time (Sec.)*
600	50	0	15	300	20	300	0
700	50	0	15	300	20	300	0

Appendix B

1. Turn of the nitrogen tank
2. Switch on TLD Reader via switch
3. Allow TLD Reader to warm up for 45 minutes
4. Connect TLD Reader USB to USB port of laptop
5. Power on laptop
6. Launch the TLD Reader program “WinREMS”
7. Click File and select “1 Reader. wrw” as your workspace
8. Click TTP on the toolbar to set up the TTP for each type of TLDs and save the TTP with a unique title.

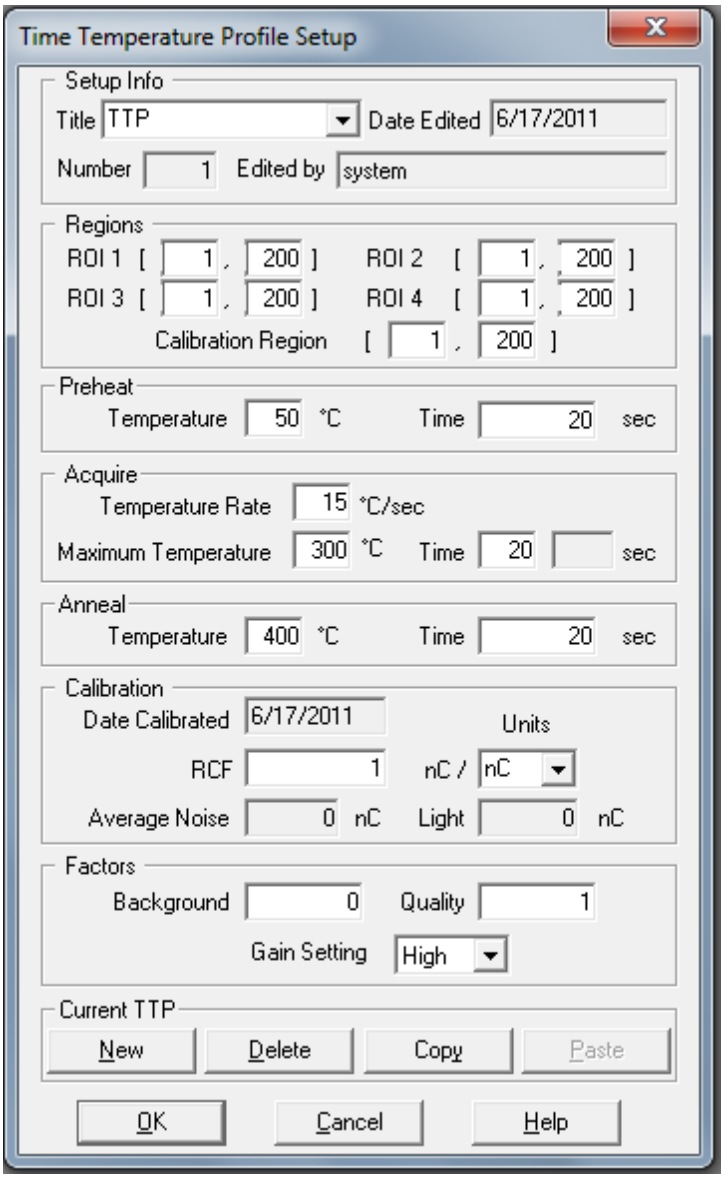
Time Temperature Profile Setup
Setup Info
Title TTP
Date Edited 6/17/2011
Number 1
Edited by system
Regions
ROI 1 [1 , 200]
ROI 2 [1 , 200]
ROI 3 [1 , 200]
ROI 4 [1 , 200]
Calibration Region [1 , 200]
Preheat
Temperature 50 °C
Time 20 sec
Acquire
Temperature Rate 15 °C/sec
Maximum Temperature 300 °C
Time 20 sec
Anneal
Temperature 400 °C
Time 20 sec
Calibration
Date Calibrated 6/17/2011
Units
RCF 1
nC / nC
Average Noise 0 nC
Light 0 nC
Factors
Background 0
Quality 1
Gain Setting High
Current TTP
New
Delete
Copy
Paste
OK
Cancel
Help

9. Chose the TTP established in step 8 for corresponding TLDs that will be read in TTP columns.

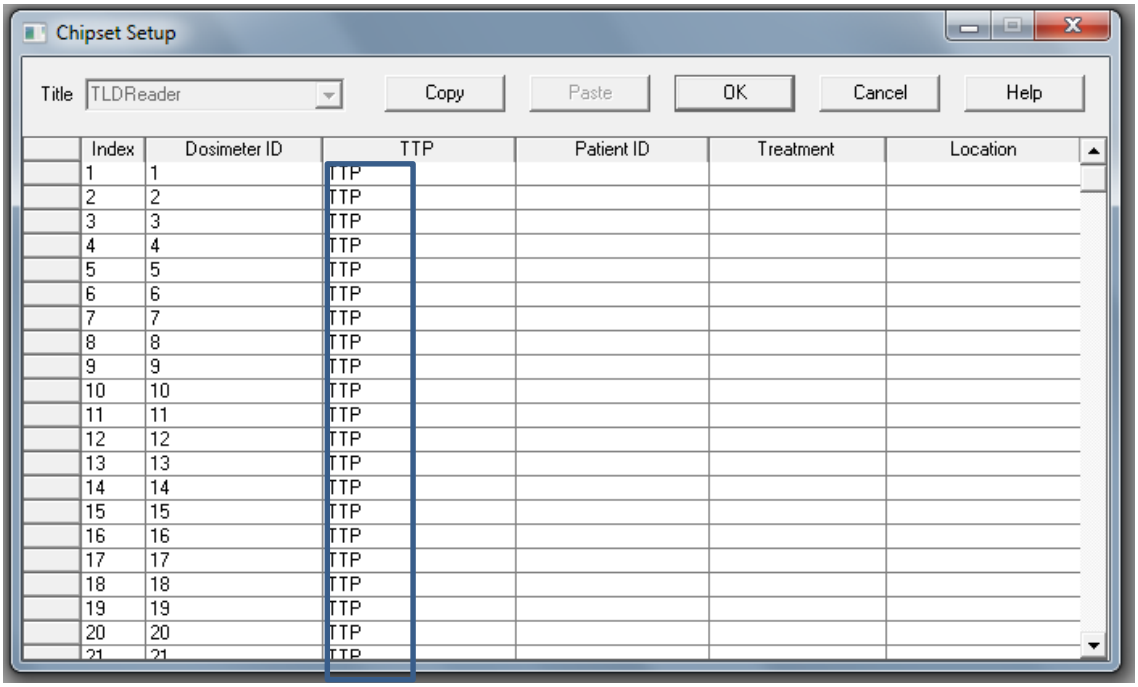

10. Load TLDs in disk holder
11. Press GO to read TLDs
12. Click RSP to access data
13. Export as ASCII file: File/export/filename/export
14. Enter data of reading on envelope
15. Turn off nitrogen tan

Appendix C

TLD ID		Calibration Factor			TLD ID		Calibration Factor		
	60 kVp	80 kVp	120 kVp	662 keV		60 kVp	80 kVp	120 kVp	662 keV
1	1.058	1.005	0.915	0.983	27	0.990	1.007	0.988	1.040
2	1.017	0.948	0.891	1.013	28	0.945	0.987	1.005	1.046
3	0.995	0.979	0.834	1.086	29	0.976	1.001	1.014	1.075
4	0.941	0.973	0.950	0.805	30	1.008	1.007	0.997	1.116
5	0.975	0.991	0.939	0.896	31	0.962	0.939	0.990	1.003
6	0.941	0.949	0.945	0.971	32	1.001	1.012	1.028	1.061
7	0.993	0.987	0.985	0.903	33	0.996	1.030	1.029	1.051
8	0.982	1.000	0.966	1.000	34	1.013	1.009	1.001	0.881
9	1.009	1.010	0.965	0.959	35	0.990	0.997	1.008	0.813
10	1.053	1.052	0.951	1.109	36	1.004	1.011	1.017	0.934
11	1.016	1.034	1.014	1.089	37	1.057	1.020	1.037	0.980
12	1.024	0.995	1.030	1.032	38	1.039	1.019	1.040	0.883
13	1.093	1.034	1.013	1.073	39	1.067	1.059	1.074	0.992
14	1.018	1.011	1.012	0.942	40	0.983	0.980	0.990	0.886
15	0.940	0.947	0.978	0.930	41	1.011	1.003	1.013	0.868
16	1.019	1.003	1.009	1.073	42	0.993	0.972	1.000	1.037
17	0.961	1.002	1.015	1.030	43	1.007	0.983	1.028	0.951
18	0.958	0.964	1.022	0.913	44	0.987	0.991	1.051	0.988
19	1.031	1.028	1.051	1.139	45	1.018	1.028	1.033	0.984
20	0.982	0.960	1.051	1.018	46	0.976	0.995	1.035	1.015
21	1.036	1.024	1.008	0.837	47	0.973	1.025	1.065	1.166
22	0.990	0.990	0.965	0.995	48	1.018	0.992	1.034	1.158
23	1.080	1.087	1.040	1.193	49	1.025	1.041	1.024	1.140
24	1.000	1.043	1.030	1.070	50	0.991	1.039	1.041	1.121
25	0.974	1.005	1.079	0.957	51	1.034	0.968	0.995	1.077
26	0.952	0.954	0.943	1.117	52	0.962	0.960	0.976	1.058

Appendix D

TLD ID		Calibration Factor			TLD ID		Calibration Factor		
	60 kVp	80 kVp	120 kVp	662 keV		60 kVp	80 kVp	120 kVp	662 keV
1	1.00374	1.00374	0.97673	0.99324	27	0.98805	1.0065	1.00535	1.01219
2	0.99401	0.99401	0.9681	0.96869	28	0.9591	0.9872	1.00865	1.01152
3	0.99519	0.99519	0.97697	0.98861	29	0.94351	1.0012	0.9796	0.9784
4	1.03561	1.03561	0.96892	1.02143	30	1.00746	1.0068	1.01738	1.02998
5	1.01623	1.01623	0.98201	1.02398	31	0.99691	0.9965	1.01454	1.02296
6	1.02628	1.02628	0.99311	1.04042	32	0.99648	0.9711	1.00422	0.99228
7	0.99605	0.99605	0.9837	0.99646	33	0.98227	0.9713	0.96939	1.00986
8	1.03375	1.03375	1.0192	1.02654	34	0.99896	0.9797	1.02076	0.94635
9	1.02174	1.02174	0.97222	1.00689	35	1.02617	1.0227	1.02324	0.96778
10	1.0248	1.0248	1.00321	0.9716	36	0.96391	0.9586	0.98068	0.91348
11	1.00494	1.03433	0.98613	0.99678	37	0.98605	1.0117	0.99163	0.97129
12	1.01477	0.99467	0.95869	0.96793	38	0.99745	0.9969	0.99016	0.977
13	1.01712	1.0342	0.96599	0.97329	39	1.05695	1.0351	1.02495	0.99292
14	1.01188	1.01086	1.00523	1.00099	40	1.04404	1.0253	1.04029	1.02757
15	1.03006	0.94676	1.04164	1.0262	41	0.98039	0.9904	0.99559	0.9834
16	0.9779	1.00307	0.98467	0.96854	42	0.99358	1.0073	1.04696	0.9285
17	1.016	1.00197	1.01544	1.02364	43	0.9906	1.0071	1.01184	0.99775
18	0.99241	0.96414	1.03477	0.99308	44	1.01166	0.9993	1.01933	1.02415
19	1.04063	1.02849	1.02429	1.05234	45	0.98248	0.9762	0.99336	0.99324
20	0.96876	0.96041	0.98153	0.97824	46	0.95671	0.9721	0.95697	0.98042
21	1.06304	1.02387	1.04737	1.00821	47	1.02083	1.0059	1.01287	1.03361
22	0.99273	0.98999	1.01377	0.98655	48	0.99187	0.9783	1.00245	1.02228
23	1.02344	1.08671	1.03557	1.02211	49	0.98018	0.9816	1.01108	1.02041
24	0.96876	1.04262	0.98881	0.98703	50	0.98605	0.9612	0.9837	0.99986
25	0.97759	1.00454	0.99509	1.00738	51	0.96332	0.9169	1.02041	1.22697
26	0.98143	0.95359	0.97924	0.98687	52				

Appendix E

Am-Be			
TLD ID	CF	TLD ID	CF
1	0.949046	27	0.947417
2	1.005584	28	0.965914
3	0.973592	29	0.95242
4	0.980223	30	0.947185
5	0.962192	31	1.015007
6	1.004886	32	0.942531
7	0.965798	33	0.926245
8	0.953699	34	0.944974
9	0.944509	35	0.956375
10	0.906701	36	0.942997
11	0.92194	37	0.935202
12	0.958702	38	0.935668
13	0.922057	39	0.900768
14	0.943346	40	0.973476
15	1.007213	41	0.950675
16	0.950675	42	0.980921
17	0.951722	43	0.969753
18	0.989065	44	0.962541
19	0.927175	45	0.927641
20	0.992904	46	0.958353
21	0.931363	47	0.9302
22	0.963239	48	0.961145
23	0.877501	49	0.915775
24	0.914611	50	0.917403
25	0.949279	51	0.985527
26	1	52	0.99366

Appendix F

Am-Be			
TLD ID	CF	TLD ID	CF
1	0.887365	27	1.039367
2	0.944614	28	1.052359
3	0.959416	29	1.008248
4	0.930262	30	1.135767
5	0.941972	31	1.070763
6	0.855794	32	0.920095
7	0.991914	33	0.869045
8	1.084557	34	0.980364
9	1.079343	35	0.976101
10	1.074178	36	0.951285
11	1.12439	37	0.97328
12	1.044201	38	0.95398
13	0.944614	39	1.025129
14	0.980364	40	1.133855
15	1.070763	41	1.028259
16	1.067369	42	1.049081
17	1.052359	43	0.960784
18	1.040973	44	0.993377
19	1.105927	45	1.069063
20	1.098711	46	1.131949
21	1.029832	47	1.050717
22	0.793298	48	1.022018
23	0.925151	49	1.209174
24	0.839788	50	1.226794
25	0.939344	51	0.834585
26	0.959416	52	

Appendix G

Radiation Survey

Background reading: 0-1μR/hr

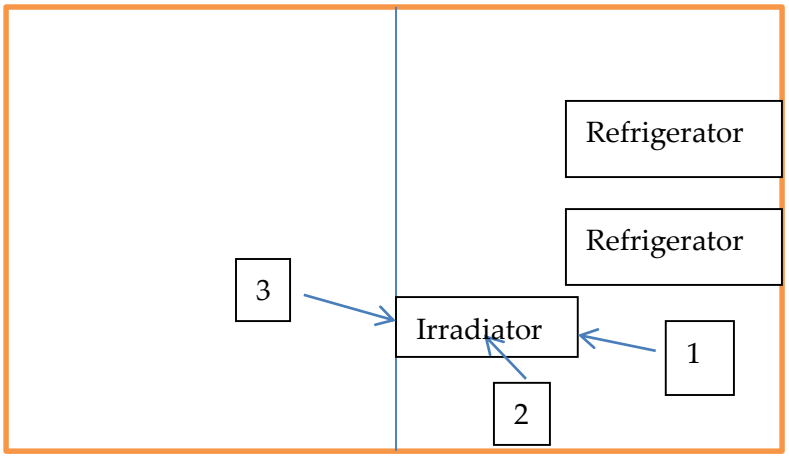

Location	kVp	mA	Time(s)	Reading(μR/hr)
1	160	18	200	0-1
2	160	18	200	8
3	160	18	200	2-4

References

[1]. Attix, F. *Introduction to Radiological Physics and Radiation Dosimetry*. WILEY-VCH Verlag GmbH & Co. KGaA, 2004.

[2]. Knoll, Glenn F. *Radiation detection and measurement (3rd ed.).* New York: Wiley, 1999.

[3]. Thermo Scientific. *Product Overview Materials and Assembies for Thermoluminescenece Dosimetry*

[4]. http://www.rti.se/products/piranha/

[5]. Samuel Loren Brady. *Development of radiatiochromic film for spatially quantitative dosimetric analysis of indirect ionizing radiation fields*. PhD's Dissertation. 2010

[6]. Yigal S. Horowitz. *Thermoluminesence and Thermoluminescent Dosimetry Dosimetry Volume III.* CRC Press, Inc., 1984

[7]. http://www.tunl.duke.edu

[8]. Brian W. Swartz. Characterization of neutron beams produced using the $^{2}H(d,n)$ reaction for determining dose to small animals. Master's Thesis. 2007

[9]. Cameron, J. R., D. Zimmerman, G. Kenney, R. Buch, R. Bland, and R. Grant. (1964). *"Thermoluminescent radiation dosimetry utilizing LiF."* Health Phys 10:25–29.

[10]. Thermo Electron Corporation. *Harshaw standard TTP Recommendations Technical Notice* publication No. DOSM-0-N-1202-001 Release Date: Dec.2, 2002

[11]. Precision. *X-RAD 320 Biological X-Ray Irradiator*

[12]. Neely Nuclear Research Center. *Calibration procedure for basic portable neutron meters, procedure 9053*

[13]. http://www.rso.wsu.edu/rppm/Am-241%20and%20Be-9.htm

[14]. Ngaile, J. E. and Muhogora, W. E. *Performance characteristics of LiF thermoluminescent dosemeters employed in the National Personnel Radiation Dose Services inTanzania*. J. Radiol. Prot. 24, 155–164 (2004).

[15]. Rossi et al. AAPM Report No. 14 *Performance Specifications and Acceptance Testing for X-ray Generators and Automatic Exposure Control Devices*. AAPM Report 14. 1985

[16]. Mohaupt et al. *Laboratory X-ray irradiator for cellular radiobiology research studies: Dosimetry report.* AFRRI TECHNICAL REPORT. 1985

[17]. Precision. *X-RAD 160 Biological X-Ray Irradiator*

[18]. Chu Wang. *Evaluation of Patient Effective Dose of Neurovascular Imaging Protocols of a C-arm Cone-beam CT & Estimation of Current Source Radioactivity of a Cs-137 Irradiator.* Master's Thesis, 2012

[19]. Natalie Januzis. *Accuracy of Effective Dose Estimation Using Single and Double Badges and an Evaluation of Organ Dose and Image Quality in Thoracic MDCT Scans Through a Comparison of Bismuth Shields and a Global Reduction in Tube Current.* Master's Thesis, 2012